ORIGINAL ARTICLE

Plant Pathology **WILEY**

Argentinian potato leafroll virus P0 protein: Novel activities for a previously known suppressor

María P. Barrios Barón[1] | Verónica C. Delfosse[1,2] | Yamila C. Agrofoglio[1] | Vanesa Nahirñak[1] | Natalia I. Almasia[1] | Cecilia Vazquez Rovere[1] (iD) | Ana J. Distéfano[1,3] (iD)

[1]Instituto de Agrobiotecnología y Biología Molecular (IABIMO), INTA-CONICET, N. Repetto y de las Cabañas s/n, Buenos Aires, Argentina

[2]School of Science and Technology, UNSAM, Buenos Aires, Argentina

[3]Universidad Nacional de Luján (UNLU), Buenos Aires, Argentina

Correspondence
Cecilia Vazquez Rovere, Instituto de Agrobiotecnología y Biología Molecular (IABIMO), INTA-CONICET, N. Repetto y de las Cabañas s/n (1686) Hurlingham, Buenos Aires, Argentina.
Email: vazquez.cecilia@inta.gob.ar

Present address
Yamila C. Agrofoglio, Centro Nacional de Biotecnología (CNB-CSIC), Madrid, Spain

Abstract

The potato leafroll virus (PLRV) P0 protein (P0^{PL}) is a suppressor of RNA silencing. In this study, we showed that P0 protein from an Argentinian isolate of PLRV (P0^{PL-Ar}) has an additional activity not described for other PLRV or P0 proteins from poleroviruses. Besides reporting that P0^{PL-Ar} displays both local and systemic silencing suppressor activity, we demonstrated, for the first time, that P0^{PL-Ar} impedes accumulation of dsRNA-derived siRNAs. We also showed that P0^{PL-Ar} interacts with *Solanum tuberosum* SKP1 orthologue (StSKP1) and triggers destabilization of ARGONAUTE 1 (AGO1) and that these actions are mediated by the F-box-like domain. A mutant in the GW/WG motif within the P0^{PL-Ar} F-box-like motif lost the suppression activity, the interaction with StSKP1 and abolished AGO1 decay. Interestingly, a mutant in the L76/P77 residues within the P0^{PL-Ar} F-box-like motif, which lost the suppression activity and the interaction with StSKP1, retained the capacity to enable AGO1 decay. Thus, unlike other P0 proteins of previously characterized poleroviruses, P0^{PL-Ar} seems to have a dual activity, according to the findings of this study. This protein would act at both an upstream and a downstream step of the RNA silencing pathway: upstream of Dicer-like enzyme (DCL)-mediated primary siRNA production and downstream at the RNA-induced silencing complex (RISC) complex level. Our results contribute to the understanding of the different ways PLRV P0 proteins function as silencing suppressors.

KEYWORDS
ARGONAUTE (AGO) decay, F-box motif, P0 protein, potato leafroll virus (PLRV), SKP1, suppressor of RNA silencing

1 | INTRODUCTION

Solanum tuberosum subsp. *tuberosum*, a solanaceous food crop commonly known as potato, is an herbaceous plant grown worldwide. Due to its nutritional properties and mode of propagation, the potato is considered the fourth most important staple crop in the world (Zaheer and Akhtar, 2016). In Argentina, approximately 75,000 ha of

potato crop are planted annually with an average production of 2.4 million tonnes (Mercado Central de Buenos Aires, 2018). Viruses are important pathogens that can substantially decrease yield and crop quality. More than 50 viruses and two viroids have been reported infecting potatoes (Kreuze et al., 2020); among them, potato leafroll virus (PLRV) and potato virus Y (PVY) are the most harmful and have a worldwide distribution (Kreuze et al., 2020).

Potato leafroll virus (PLRV) is the type member of the genus *Polerovirus* within the family *Luteoviridae*, which is a group of phloem-limited plant

C. Vazquez Rovere and A. J. Distéfano contributed equally to this work.

viruses transmitted efficiently by a restricted number of aphid species (Domier, 2012). In particular, the green peach aphid, *Myzus persicae*, is the most efficient and important PLRV vector (Mondal et al., 2017). A reported isolate of Argentinian PLRV has a monopartite positive-sense RNA genome of about 5.9 kb with 10 open reading frames (ORFs) (Barrios Barón et al., 2017). This virus is distributed within all major potato-growing regions of Argentina affecting yield and tuber quality, and causes one of the most important potato diseases causing losses of up to 90% of the crop (https://www.sinavimo.gov.ar/plaga/potato-leafroll-virus).

In plants, RNA silencing constitutes an important mechanism of innate immunity for defence against viral infections (Csorba et al., 2015). It is triggered by viral double-stranded RNA (dsRNA) produced during the replication of viruses. Once the mechanism is triggered, the viral dsRNA is processed by Dicer-like (DCL) enzymes into short interfering RNAs (siRNAs) of 21–24 nucleotides (Ding, 2010). One strand of the viral siRNA duplex is loaded into a distinct ARGONAUTE protein (AGO)-containing effector complex, called the RNA-induced silencing complex (RISC), to guide sequence-specific degradation of the viral RNA target molecules (Vaucheret, 2008). To counteract this host defence mechanism, viruses have evolved a great diversity of proteins, viral suppressors of RNA silencing (VSRs), that can block RNA silencing at different steps of the pathway (Csorba et al., 2015). Inhibiting dsRNA processing or hijacking siRNAs are common mechanisms of VSRs used by positive-strand RNA viruses to inhibit RISC assembly and interfere with systemic silencing (Qu et al., 2003; Lakatos et al., 2006; Schuck et al., 2013). Other viral suppressors interfere with RNA silencing through the direct or indirect interaction with different components of the RISC (Csorba et al., 2015).

For several viruses of the genus *Polerovirus*, the P0 protein, which is encoded by the open reading frame (ORF) most proximal to the 5′ end of the genome, has been reported as a suppressor of RNA silencing with different activity levels according to the species (Pazhouhandeh et al., 2006; Mangwende et al., 2009; Han et al., 2010; Kozlowska-Makulska et al., 2010; Liu et al., 2010; Fusaro et al., 2012; Delfosse et al., 2014; Zhuo et al., 2014; Chen et al., 2016; Wang et al., 2018; Agrofoglio et al., 2019; Li et al., 2019). The amino acid sequence identity of polerovirus P0 proteins is very low, with an average value of 37.1%. Despite the differences in sequence, most P0 proteins contain a conserved F-box-like motif required for the P0's silencing suppressor activity (Pazhouhandeh et al., 2006). Through this motif, some P0s interact with S-phase kinase-related protein-1 (SKP1), a subunit of the SCF family of E3 ubiquitin ligases, and promote ubiquitination and degradation of ARGONAUTE 1 (AGO1) (Derrien et al., 2012).

The silencing-suppressor activity described for the P0 protein of PLRV (P0^{PL}) varies among different PLRV isolates. So far, P0^{PL} proteins of isolates from Europe, Inner Mongolia, Australia, and Canada have been shown to have RNA silencing suppressor activity, with different suppression intensities at the local level (Pazhouhandeh, 2007; Fusaro et al., 2012; Zhuo et al., 2014; Rashid et al., 2019). Moreover, P0^{PL} proteins of isolates showed differences regarding their interaction with E3 SCF ubiquitin ligase complexes.

For example, the Inner Mongolian P0^{PL} does not interact with *Nicotiana benthamiana* SKP1 (NbSKP1) (Zhuo et al., 2014), whereas the European P0^{PL} interacts weakly with NbSKP1 and not with *Arabidopsis thaliana* orthologues ASK1 and ASK2 (Pazhouhandeh, 2007). Interestingly, the Inner Mongolian PLRV P0 protein (P0^{PL-IM}) has an unusual F-box between amino acids 76 and 95 with a tryptophan/glycine (WG) sequence, and possesses an additional GW/WG-like motif (G139/W140/G141), absent in other poleroviral P0 proteins (Zhuo et al., 2014). The mutation of amino acids L76, W87, or G88 in the F-box as well as of the residue F220 in the C-terminal conserved region abolished P0^{PL-IM} suppressor activity (Zhuo et al., 2014). Furthermore, the replacement of W140A in the G139/W140/G141-like motif weakened P0 activity (Zhuo et al., 2014). Recently, Rashid et al. (2019) confirmed these findings for a Canadian P0^{PL} and revealed that the VSR-defective mutants in the F-box-like motif, the G139/W140/G141-like motif, and in the C-terminus of P0 (F220) affected not only virus accumulation but also its systemic movement. With these results, Rashid et al. (2019) demonstrated that P0 is required for PLRV accumulation and systemic infection.

The aim of this study was to characterize the suppressor activity of the P0 protein of an Argentinian isolate (P0^{PL-Ar}), using different approaches and techniques. We investigated the intensity of silencing suppression, the interactions of P0^{PL-Ar}, and the steps of the silencing pathway on which the P0^{PL-Ar} acted.

2 | MATERIALS AND METHODS

2.1 | Plasmid constructs

To obtain the ORF0 of the Argentinian isolate of PLRV (PLRV-Ar, GenBank accession number KY856831), total RNA was isolated from PLRV-infected potato leaf tissue using TriPure isolation reagent (Roche). cDNA was synthesized with 3 µg of total RNA and SuperScript III reverse transcriptase (Thermo Fisher Scientific) according to the manufacturer's instructions. ORF0 was amplified by PCR using PL pP0Up2 and PL P0Low3 primers (Table S1). The PCR was performed with USB FidelityTaq PCR Master Mix (2×) (Affymetrics) and was carried out with a denaturation step at 95°C for 1 min; followed by 35 cycles of 30 s at 94°C, 30 s at 55°C, and 1 min at 68°C; with a final extension at 68°C for 5 min. The amplified product was purified using QIAEX II Gel Extraction kit (QIAGEN), cloned into pGEM-T Easy vector according to the manufacturer's instructions (Promega) and sequenced using an ABI 3730 XL automated sequencer. The fragment was digested with *Xba*I and *Bam*HI restriction enzymes and subcloned into pBin61 binary vector to produce pBin61-P0^{PL-Ar}. ORF0 of a European isolate of PLRV (PLRV-NL), cloned into pBin61, was kindly provided by Dr. Véronique Ziegler-Graff of IBMP, Strasbourg, France.

Single base change mutations in the gene for P0 were obtained by the overlap extension PCR technique using pBin61-P0^{PL-Ar} as a template. P0 was amplified in two fragments, where PL pP0up

(forward primer) was combined with either pP0PL lp R or pP0PL wg R (reverse primers), depending on the mutation to be generated (P0$^{PL-Ar-LP(76-77)AA}$ or P0$^{PL-Ar-WG(87-88)AA}$, respectively) to obtain the 5′ portion, whereas PL pP0low was combined with either pP0PL lp F or pP0PL wg F primers, to obtain the 3′ portion. Then, the complete mutated P0s were amplified using first round products as templates (in a molar ratio of 1:1) and PL pP0up and PL pP0low primers. All PCRs were performed with USB FidelityTaq PCR Master Mix (2×) (Affymetrics). Amplifications were carried out with a denaturation step at 95°C for 1 min; followed by 35 cycles of 30 s at 94°C, 30 s at 55°C, and 1 min at 68°C; with a final extension at 68°C for 5 min. All primer sequences are listed in Table S1.

Subsequently, c-Myc-tagged P0 proteins were obtained by using P0$^{PL-Ar- LP(76-77)AA}$ and P0$^{PL-Ar-WG(87-88)AA}$ mutants as templates and GW pP0PL F and GW pP0PL R primers. PCRs were performed with USB FidelityTaq PCR Master Mix (2×) (Affymetrics). Amplifications were carried out with a denaturation step at 95°C for 1 min; followed by 35 cycles of 30 s at 94°C, 30 s at 65°C, and 1 min at 68°C; with a final extension at 68°C for 5 min. PCR products were gel purified with QIAEX II (QIAGEN) and recombined into pDONR/Zeo vector by performing a BP recombination reaction with Gateway BP Clonase II enzyme mix (Thermo Fisher Scientific) according to the manufacturer's instructions. As described by Agrofoglio et al. (2019), all the clones obtained were sequenced and recombined into a pGWB617 Gateway destination vector (Nakamura et al., 2010) by LR recombination reaction with Gateway LR Clonase II enzyme mix (Thermo Fisher Scientific), according to the manufacturer's protocol. Finally, recombinant vectors were introduced into *Agrobacterium tumefaciens* GV3101 by electroporation.

2.2 | Agroinfiltration assays

Plants of *Nicotiana benthamiana* wild type and *N. benthamiana* line16c, which is homozygous for the green fluorescent protein (GFP) transgene, were grown in soil in greenhouses or breeding chambers, under controlled conditions of 24 ± 1°C, with a photoperiod of 16 hr of light and 8 hr of darkness.

Every agroinfiltration assay consisted of coinfiltrating four or five leaves of 10 *N. benthamiana* plants or 10 *N. benthamiana* line 16c plants (3 weeks old) with a mixture of *A. tumefaciens* GV3101 cultures harbouring a sense GFP inducer (pBin61-GFP) plus one of the following vectors: pBin61 empty vector as a negative control, pBin61-P0^{Tu} and pBin61-P0^{CL} as positive controls, pBin61-P0^{PL-NL} and pBin61-P0^{PL-Ar}. Noninfiltrated 16c plants were used as a control. For coinfiltrations, equal volumes of each *A. tumefaciens* GV3101 culture were grown at 28°C in Luria Bertani (LB) medium supplemented with antibiotics according to the resistance carried by the vector. Cells were collected by centrifugation, resuspended in infiltration buffer (10 mM MES pH 5.7, 10 mM MgCl$_2$, 150 μM acetosyringone) and individually diluted to OD$_{600}$ of 1. pBin61-GFP culture was mixed with pBin61 empty vector, pBin61-P0^{Tu}, pBin61-P0^{CL},

pBin61-P0^{PL-NL}, or pBin61-P0^{PL-Ar} prior to agroinfiltration to a final OD$_{600}$ of 0.5 and incubated at room temperature for at least 3 hr. Each agroinfiltration experiment was performed at least three times. For local silencing assays, the GFP fluorescence was monitored at 5 days postinfiltration (dpi), while for systemic silencing assays, the GFP fluorescence was monitored at 18 dpi. GFP fluorescence was monitored by illumination with a hand-held UV light source. Leaves and whole plants were photographed under UV light using a Canon Power Shot SX50 HS digital camera.

AGO1 destabilization was evaluated in four independent assays by infiltrating *N. benthamiana* leaves with *A. tumefaciens* containing the vectors pBinGFP-AGO1 (OD$_{600}$ 0.5), pBinP19 (OD$_{600}$ 0.25), and each version of the P0 protein (OD$_{600}$ 0.5). The inoculated leaves were harvested 3 dpi for western blot analysis. The vectors pBinGFP, pBin-GFFG, pBinP19, and pBinGFP-AGO1 have been previously described by Himber et al. (2003).

2.3 | Yeast two-hybrid assays and bimolecular fluorescence complementation

ORF0^{PL-Ar} was amplified by PCR using PLa P0 D/PLa P0 D2 and PLa P0 R P0 primers (Table S1) and P0 constructs described above were used as templates. The PCRs were performed with USB FidelityTaq PCR Master Mix (2×) (Affymetrics) and carried out with a denaturation step at 95°C for 1 min; followed by 35 cycles of 30 s at 94°C, 30 s at 55°C, and 1 min at 68°C; with a final extension at 68°C for 5 min. Forward primers lacked the initiation codon and both primers, forward and reverse, contained restriction sites. The obtained fragments were gel purified using QIAEX II Gel Extraction kit (QIAGEN) and cloned into pGEM-T Easy vector (Promega) according to the manufacturer's protocol, sequenced, and excised using *Eco*RI/*Nco*I and *Spe*I/*Bam*HI restriction enzymes. Subsequently, the fragments were subcloned into pGADT7 or pGBKT7 (TaKaRa Bio Inc.) according to the manufacturer's instructions. The ORF for StSKP1 of *S. tuberosum* (GenBank: XM_006362658.2), which lacks the translation initiation codon, was amplified by PCR with specific primers St SKP1 D and St SKP1 R (Table S1) and *S. tuberosum* 'Kennebec' cDNA as template under the same conditions described above for the ORF0^{PL-Ar}. The amplified products were gel-purified using QIAEX II Gel Extraction kit, subsequently cloned into pGEM-T Easy vector (Promega), sequenced and finally transferred into yeast two-hybrid (Y2H) vectors pGBKT7 or pGADT7. *A. thaliana* S-phase kinase-related proteins ASK1 and ASK2, in Y2H vectors (pGAD-ASK1, pGBK-ASK1, pGAD-ASK2, pGBK-ASK2), as well as *N. benthamiana* S-phase kinase-related protein 1, NbSKP1, in Y2H vectors (pGAD-NbSKP1 and pGBK-NbSKP1) were kindly provided by Dr. Véronique Ziegler-Graff and have been previously described by Pazhouhandeh et al. (2006). The vector pLAW10-NbSKP1 was kindly provided by Dr. Gabriela Llauger.

Y2H assays were performed as suggested by the Clontech Matchmaker Protocol with *Saccharomyces cerevisiae* AH109. Protein interaction in double-transformed yeast was analysed on synthetic defined (SD) medium lacking adenine, histidine, tryptophan, and leucine (−AHWL). Plates were incubated at 21 or 28°C when indicated.

FIGURE 1 Silencing suppression activity and molecular characterization of P0^{PL-Ar} protein. (a) Leaves of *Nicotiana benthamiana* line 16c were coinfiltrated with a mixture of *Agrobacterium tumefaciens* cultures harbouring a sense green fluorescent protein (GFP) inducer plus one of the following vectors: pBin61 empty vector as a negative control (panel B), P0^{Tu} (panels C and G) and P0^{CL} (panels D and H) as positive controls, P0^{PL-NL} (panel E) and P0^{PL-Ar} (panel F and I). Noninfiltrated (NI) 16c plants (panel A) were used as a control. Arrows indicate the red halo bordering the infiltration patch. Photographs were taken under UV light 5 days postinfiltration (dpi). (b) GFP fluorescence from three independent assays was quantified by fluorescence spectrometry and normalized to GFP plus pBin61. The average amount is shown with standard deviations as error bars. Asterisks indicate significant differences between treatments (*.01 < p < .05, **.001 < p < .01). (c) Northern blot analysis of total RNA extracted from *N. benthamiana* 16c leaves at 5 dpi infiltrated with a mixture of *A. tumefaciens* cultures harbouring a sense GFP inducer plus: pBin61 empty vector (lane 2), P0^{Tu} (lane 3), P0^{CL} (lane 4), P0^{PL-NL} (lane 5), or P0^{PL-Ar} (lane 6). NI leaves were included in the analysis (lane 1). A GFP probe was used to detect the levels of GFP mRNA and siRNA. Ethidium bromide-stained rRNA or low-molecular-weight (LMW) RNAs were used as loading control. Relative abundance (RA) data were calculated relative to GFP plus pBin61 mRNA or siRNA accumulation, which was set arbitrarily to 1. (d) Western blot analysis of total proteins from infiltrated leaves using anti-GFP monoclonal antibodies for detection of GFP protein. Ponceau S staining of the large subunit of RuBisCO protein was used as loading control. RA data were calculated relative to GFP protein accumulation in plants infiltrated with the GFP vector plus empty pBin61, which was arbitrarily set to 1. M: prestained protein marker. (e) Leaf photographs taken under normal light at 15 dpi show the cell death phenotype caused by P0^{PL-NL} (panel B) and P0^{PL-Ar} (panel C) compared to 16c plants infiltrated with pBin61 empty vector (panel A). (f) Systemic RNA silencing suppression assay. *N. benthamiana* 16c plants were infiltrated with mixtures harbouring a sense GFP inducer plus: pBin61 empty vector (panel B), P0^{Tu} (panel C), P0^{CL} (panel D), P0^{PL-NL} (panel E), and P0^{PL-Ar} (panel F). NI 16c plants (panel A) were used as a control. Photographs of whole plants were taken under UV light 18 dpi. The proportion of plants with the phenotype shown in each panel is indicated [Colour figure can be viewed at wileyonlinelibrary.com]

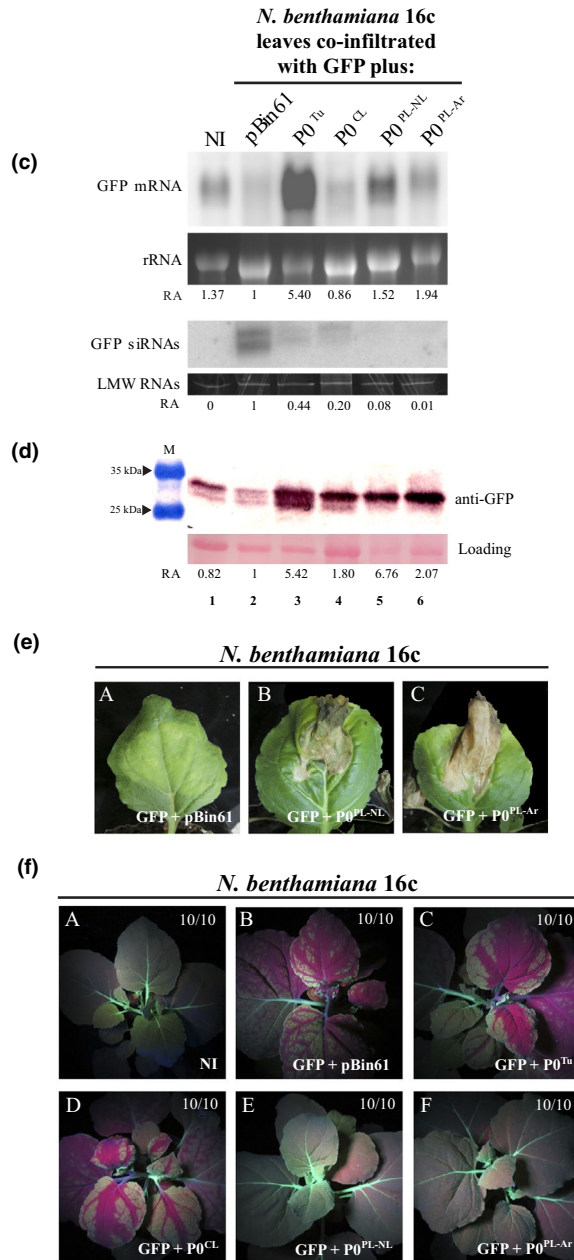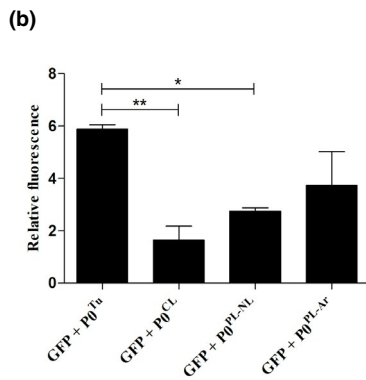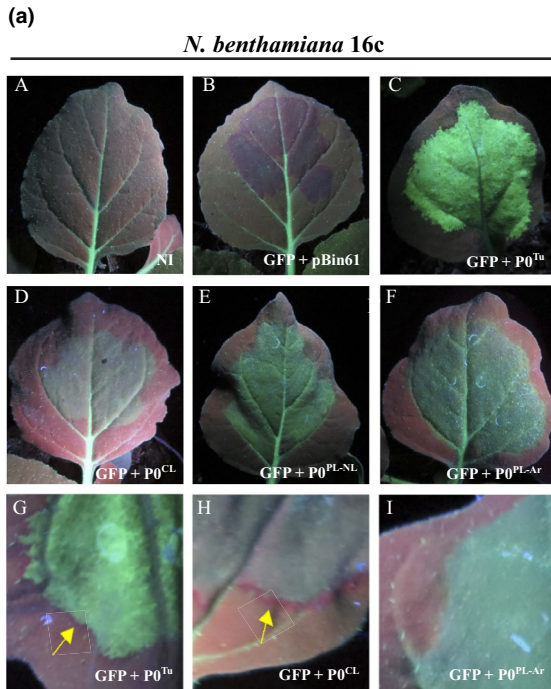Yeast colonies capable of growing on the auxotrophic medium were photographed.

For bimolecular fluorescence complementation (BiFC) analysis, ORF0^{PL-Ar} was amplified using P0^{PL-Ar} BIFC F and P0^{PL-Ar} BIFC R primers and pBin61-P0^{PL-Ar} as template. StSKP1 was amplified using StSKP1 BIFC F and StSKP1 BIFC R primers and pGEMT-StSKP1 as template (Table S1). Each PCR was performed with USB FidelityTaq PCR Master Mix (2×) (Affymetrics). Amplifications were carried out with a denaturation step at 95°C for 1 min; followed by 35 cycles of 30 s at 94°C, 30 s at 54°C, and 1 min at 68°C; with a final extension at 68°C for 5 min. PCR fragments were purified as described above and cloned into TOPO Gateway vector (Invitrogen) and then recombined into binary BiFC-Gateway destination vectors pDEST–VYNE(R)GW or pDEST–VYCE(R)GW (Gehl et al., 2009). *A. tumefaciens* GV3101 strains transformed with the two BiFC plasmids, containing P0^{PL-Ar} or StSKP1 and pBin-P19 (to avoid RNA silencing of the exogenous transcripts and ensure its correct expression during transient expression assay) were grown overnight in 10 ml of LB borth (supplemented with gentamycin, rifampicin, and kanamicin). The culture was pelleted and resuspended in 10 mM MES in the presence of 100 μM acetosyringone (adjusted to OD$_{600}$ 0.6) and incubated for 3 hr in darkness. Young leaves of 3–4 week-old *N. benthamiana* plants were coinfiltrated with an equal mix of both cultures. For this assay, as previously described by Nahirñak et al. (2019), StDIM/DWF1 fused at its carboxy-terminus to the two fragments (N- or C-terminal) of the Venus protein in combination with Snakin-1 fused to the C-terminal or the N-terminus fragment of Venus as C-terminal protein fusion were used as positive controls. StDIM/DWF combined to N- or C- terminal of Venus fused to Snakin-1 at its N-terminus were used as negative controls (data not shown). Abaxial epidermal cells of infiltrated leaves were analysed for fluorescence at 2–3 dpi and images were acquired under a TCS-SP5 confocal microscope (Leica Microsystems, Germany; at Laboratorio Integral de Microscopía, CICVyA, INTA) using a 63× water immersion objective.

2.4 | RNA extraction, cDNA synthesis, and northern blot assays

Leaf discs (0.5 cm diameter) from agroinfiltrated leaves of *N. benthamiana* or *N. benthamiana* line 16c were collected at 5 dpi. Twelve discs were ground with TissueLyser LT (QIAGEN) and total RNA was extracted using TriPure isolation reagent (Roche) according to the manufacturer's instructions. Total RNA was extracted from 75–100 mg of potato leaf tissue ground in liquid nitrogen using TriPure reagent according to the manufacturer's instructions with the addition of an extra step of extraction with chloroform to improve the purity of the RNA obtained.

For cDNA synthesis, RNA was treated with DNase I (Thermo Fisher Scientific) and cDNA was synthesized using random primers and SuperScript III reverse transcriptase (Thermo Fisher Scientific) according to the manufacturer's instructions.

High-molecular-weight RNA was analysed by resolving between 6 and 10 μg of total RNA on 1% agarose gels, whereas small RNA was evaluated by resolving 10 μg of total RNA on 17.5% polyacrylamide-8 M urea gels. High-molecular-weight and small RNA were then transferred to Hybond-NX membrane (GE Healthcare). In both cases, RNA samples were adjusted to the same concentration by spectrometry before electrophoresis. The relative abundance (RA) data of mRNA or siRNA was calculated relative to mRNA or siRNA accumulation in plants infiltrated with the GFP vector plus empty pBin61 (which was arbitrarily set to 1) using ImageJ software (National Institutes of Health). GFP, GF, and P probes were amplified with the combination of GFP1 with GFP8, GFP1 with GFP4, and GFP5 with GFP8 primers, respectively, (Table S1) and fragments were radiolabelled with [α-32P]-dCTP using the Prime-a-Gene Labeling System (Promega). Hybridizations were performed as previously described (Han et al., 2010).

(a) *N. benthamiana* 16c

A NI
B GFP + pBin61
C GFP + P0Tu
D GFP + P0CL
E GFP + P0PL-NL
F GFP + P0PL-Ar
G GFP + P0Tu
H GFP + P0CL
I GFP + P0PL-Ar

(b)

(c) *N. benthamiana* 16c leaves co-infiltrated with GFP plus:

	NI	pBin61	P0Tu	P0CL	P0PL-NL	P0PL-Ar
GFP mRNA						
rRNA						
RA	1.37	1	5.40	0.86	1.52	1.94
GFP siRNAs						
LMW RNAs						
RA	0	1	0.44	0.20	0.08	0.01

(d)

| | | | | | | | anti-GFP |
| Loading |
| RA | 0.82 | 1 | 5.42 | 1.80 | 6.76 | 2.07 |
| | 1 | 2 | 3 | 4 | 5 | 6 |

35 kDa, 25 kDa

(e) *N. benthamiana* 16c
A GFP + pBin61
B GFP + P0PL-NL
C GFP + P0PL-Ar

(f) *N. benthamiana* 16c
A NI 10/10
B GFP + pBin61 10/10
C GFP + P0Tu 10/10
D GFP + P0CL 10/10
E GFP + P0PL-NL 10/10
F GFP + P0PL-Ar 10/10

2.5 | Protein extraction, western blot, and GFP fluorescence quantification

Total plant proteins were extracted from four infiltrated leaf discs using denaturing buffer (65 mM Tris-HCl pH 7.8, 4 M urea, 10 mM dithioerythritol, and 0.5% [wt/vol] bromophenol blue) and separated on either 8% (for AGO1 detection) or 12% SDS-polyacrylamide gels before blotting on nitrocellulose Hybond ECL membrane (GE Healthcare). P0 proteins and AGO1-GFP were detected using an anti-cMyc mouse monoclonal primary antibody and anti-GFP mouse monoclonal primary antibody (Thermo Fisher Scientific), respectively. For GFP suppression experiments, detection was performed using a secondary antimouse antibody conjugated with alkaline

phosphatase (Merck) and NBT/BCIP reagents (Promega). On the other hand, AGO1 decay assay detection was performed using a secondary antimouse horseradish peroxidase antibody (1:5,000) and bands were visualized with the Pierce ECL Western Blotting Substrate chemiluminescence reagents (Thermo Fisher Scientific).

GFP fluorescence quantification was performed by spectrometry as described previously by Agrofoglio et al. (2019). Total proteins were extracted from the infiltrated area, with an extraction buffer (100 mM KCl, 5 mM MgCl$_2$, 400 mM sucrose, 100 mM Tris–HCl pH 8, 10% glycerol, 2 mM PMSF, complete EDTA-free protease inhibitor cocktail [Sigma-Aldrich]). Protein concentration was determined using a protein assay kit (Bio-Rad). Fluorescence detection was performed with 10 µg total protein and measured using a SpectrMax GEMINIEM

spectrofluorometer (Molecular Devices Corp.). For statistical analysis, three independent experiments were conducted for all assays. All data are presented as the average amount with standard deviations as error bars. Groups were compared by one-way analysis of variance together with Bonferroni's post hoc test using Graphpad Prism software. Statistical significance was set at a value of $p < .05$.

3 | RESULTS

3.1 | P0^{PL-Ar} is an RNA silencing suppressor that blocks the short-distance movement of the silencing signal and suppresses systemic silencing

To evaluate the capacity of P0^{PL-Ar} to suppress RNA silencing, we performed *A. tumefaciens* transient expression of GFP on *N. benthamiana* 16c plants (Ruiz et al., 1998). P0^{PL-Ar} protein suppressor ability was tested in *Agrobacterium*-infiltrated *N. benthamiana* 16c leaves in comparison with P0 proteins of turnip yellows virus (TuYV), PLRV European isolate, and cotton leafroll dwarf virus (CLRDV) (P0^{Tu}, P0^{PL-NL}, and P0^{CL}, respectively). This selection was based on the type of suppressor of RNA silencing activity that they have according to previous reports: strong, weak, and very weak suppressors for P0^{Tu}, P0^{PL-NL}, and P0^{CL}, respectively (Pazhouhandeh, 2007; Delfosse et al., 2014).

At 5 dpi patches inoculated with P0^{PL-Ar} displayed GFP fluorescence, thus indicating that P0^{PL-Ar} is a suppressor of RNA silencing. Green fluorescence intensity was comparable with that emitted from leaves infiltrated with P0^{PL-NL} and was intermediate between the fluorescence intensity of leaves agroinfiltrated with P0^{Tu} and P0^{CL} (Figure 1a,b). As expected, there was no GFP fluorescence in leaf patches agroinfiltrated with the GFP inducer alone or pBin61 empty vector (Figure 1a). Quantification of GFP fluorescence by spectrometry confirmed visual observations and furthermore demonstrated that the observed differences were significant (Figure 1b).

To confirm the above results, we subsequently performed northern and western blot analyses with total RNA and protein extracted at 5 dpi from agroinfiltrated patches. Northern blots revealed that GFP mRNA levels in leaves agroinfiltrated with GFP inducer plus P0^{PL-Ar} or P0^{PL-NL} were lower than in leaves agroinfiltrated with GFP inducer plus P0^{Tu} but higher than in leaves agroinfiltrated with GFP inducer plus P0^{CL} (Figure 1c upper panel). Western blot analyses of GFP protein accumulation in patches coinfiltrated with GFP inducer, pBin61, or GFP inducer plus the different suppressor proteins revealed that GFP protein levels were consistent with visual observation of GFP fluorescence and mRNA levels (Figure 1d).

To confirm whether P0^{PL-Ar} affects accumulation of GFP-specific siRNAs, we analysed the amount of these species in plants agroinfiltrated with pBin61-P0^{PL-Ar} or with the other suppressor proteins described above, plus GFP inducer (Figure 1a). No GFP-derived siRNAs of 21- to 24-nt were detected in plants infiltrated with GFP inducer plus either P0^{PL-Ar} or P0^{PL-NL} compared to leaves

infiltrated with P0^{Tu} and P0^{CL} (Figure 1c lower panel). Taken together, these results demonstrate that P0^{PL-Ar} is a local RNA silencing suppressor.

In our assays, both P0^{PL-NL} and P0^{PL-Ar} proteins triggered a cell death phenotype in the agroinfiltration area that was visible to the naked eye at 3 dpi and a severe necrosis was evident at 15 dpi (Figure 1e). Neither control plants inoculated with pBin61 empty vector nor plants inoculated with P0^{Tu} or P0^{CL} showed this phenotype (data not shown). Thus, this response is specific to certain PLRV P0 proteins and not to *A. tumefaciens* per se.

The effect of P0^{PL-Ar} on short-distance movement of GFP-derived siRNAs was determined by monitoring the halo formation in 16c leaves coinfiltrated with GFP inducer and the analysed suppressor proteins (Figure 1a, panels G, H, and I). At 5 dpi, leaves agroinfiltrated with GFP and the empty vector exhibited a clear red halo around the infiltration patch, which intensified over time (Figure 1a, panel B). Thus, the silencing signal was moving to contiguous cells. Consistent with data obtained by Delfosse et al. (2014), leaves infiltrated with P0^{Tu} and P0^{CL} exhibited red halos around the infiltrated patches (Figure 1a, panels G and H). In contrast, leaves infiltrated with P0^{PL} proteins showed no red halo around patches, even up to 20 dpi, suggesting that both P0^{PL-Ar} and P0^{PL-NL} block short-distance movement of siRNAs (Figure 1a, panels E, F, and I).

Some silencing suppressor proteins from viruses are able to block systemic movement of the silencing signal. In *N. benthamiana* 16c plants, this is evidenced by the GFP silencing observed in the proximal vein of newly emerging leaves. Infiltrated plants mentioned above were therefore monitored within two and a half weeks postinfiltration under UV light. All plants coinfiltrated with GFP inducer and P0^{Tu}, P0^{CL}, or pBin61 empty vector showed GFP silencing in veins of the upper leaves (Figure 1f, panels B, C, and D). However, none of the plants infiltrated with GFP inducer and P0^{PL-Ar} or P0^{PL-NL} showed systemic GFP silencing in upper leaves (Figure 1f, panels E and F). This indicates that P0 proteins of the Argentinian and European isolates of PLRV are able to inhibit the long-distance movement of the RNA silencing signal.

3.2 | P0^{PL-Ar} interferes with primary siRNA accumulation

To identify the step in the silencing pathway in which P0^{PL-Ar} interferes, we analysed the effect of P0^{PL-Ar} on the generation of primary and secondary siRNA species in an inverted repeat post-transcriptional gene silencing (IR-PTGS) assay. In a first approach, *N. benthamiana* leaves were agroinfiltrated with a mixture of cultures of *A. tumefaciens* harbouring the vector pBin61-GFFG (GFFG is a dsRNA silencing inducer with only the 5' half of the GFP gene) plus P0^{PL-Ar}, P0^{PL-NL}, P0^{Tu}, P0^{CL}, P38^{TCV} (P38^{TCV} is the VSR of turnip crinkle virus, *Carmovirus*), or pBin61 empty vector. P0 proteins of TuYV, CLRDV, and P38^{TCV} were used as controls. P0^{Tu} or P0^{CL} were selected because they do not inhibit the processing of dsRNA whereas P38^{TCV} does (Qu et al., 2003). Primary siRNAs

N. benthamiana leaves co-infiltrated with GFFG plus:

(a)

GF siRNAs

LMW RNAs

	pBin61	P0^{Tu}	P0^{CL}	P0^{PL-NL}	P0^{PL-Ar}	P38^{TCV}
RA	1	1.58	1.2	0.48	0.25	0.2
	1	2	3	4	5	6

N. benthamiana leaves co-infiltrated with:

GFP + GFFG plus:

(b)

GFP mRNA

rRNA

	NI	GFP + pBin61	pBin61	P0^{Tu}	P0^{CL}	P0^{PL-NL}	P0^{PL-Ar}
RA	0.1	1	0.7	10	2.11	5.15	5.1

GF siRNAs

LMW RNAs

RA	0.02	1	2.5	1.51	1.34	0.89	0.4

P siRNAs

LMW RNAs

RA	0.02	1	0.96	0.09	0.01	0.003	0.008

(c)

anti-GFP

Loading

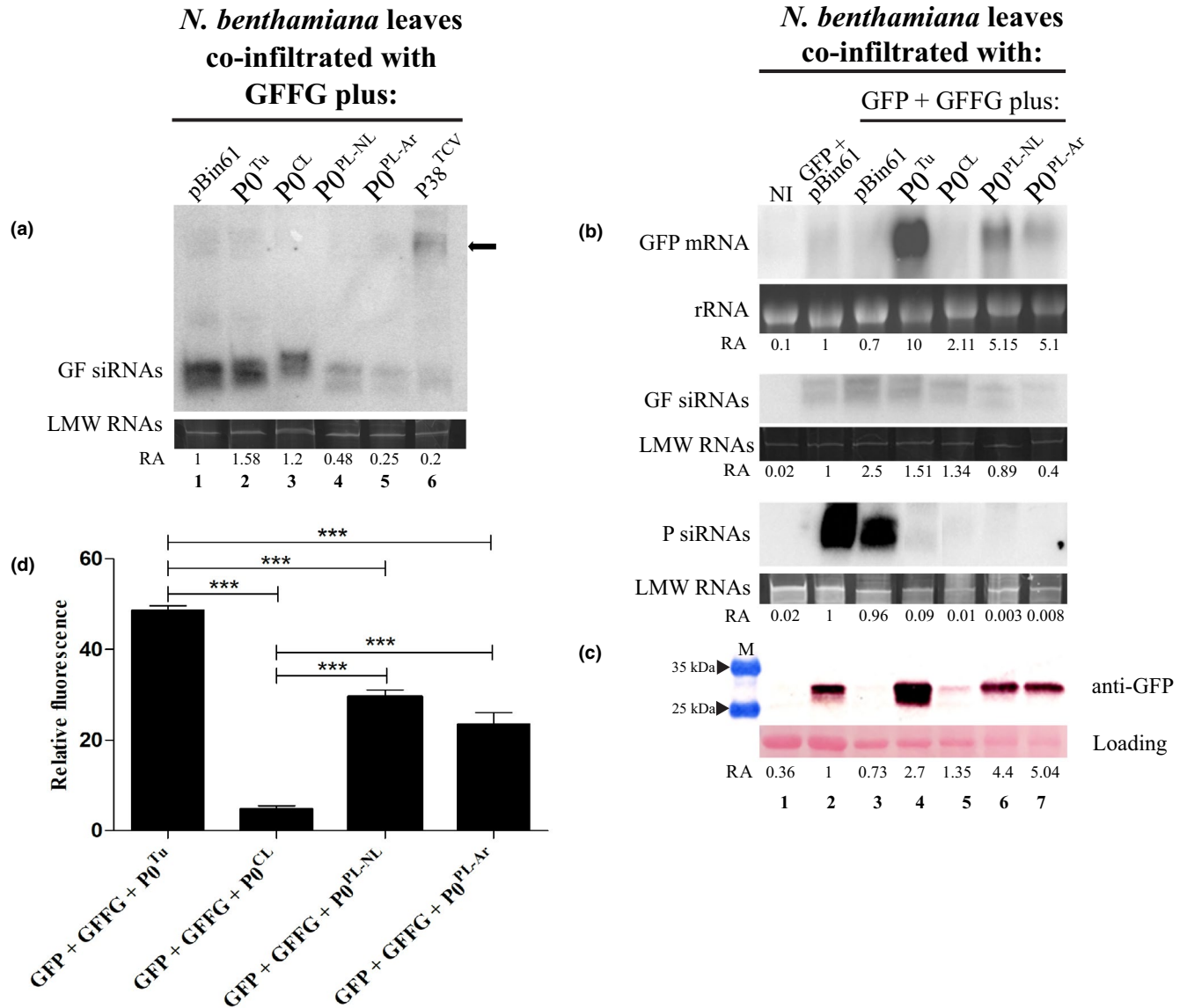|							
RA	0.36	1	0.73	2.7	1.35	4.4	5.04
	1	2	3	4	5	6	7

(d)

FIGURE 2 P0^{PL-Ar} suppresses silencing triggered by an inverted-repeat sequence. (a) *Nicotiana benthamiana* leaves were coinfiltrated with a mixture of *Agrobacterium tumefaciens* cultures harbouring a dsRNA inducer "GFFG" plus one of the following vectors: pBin61 empty vector (lane 1), P0^{Tu} (lane 2) and P0^{CL} (lane 3) as positive controls, P0^{PL-NL} (lane 4), P0^{PL-Ar} (lane 5), and P38^{TCV} as a negative control. Total RNA was extracted and analysed for the presence of GF small RNA with a GF probe by northern blot. Ethidium bromide-stained low-molecular-weight (LMW) RNAs were used as loading control. Relative abundance (RA) data were calculated relative to GF siRNA accumulation in *N. benthamiana* plants agroinfiltrated with GFFG plus the empty vector pBin61, which was arbitrarily set to 1. The arrow indicates high molecular weight dsRNA. (b) Leaves of *N. benthamiana* were infiltrated with a mixture of agrobacteria containing sense GFP and GFFG plus either pBin61 (lane 3), P0^{Tu} (lane 4) and P0^{CL} (lane 5) as positive controls, P0^{PL-NL} (lane 6) and P0^{PL-Ar} (lane 7). The green fluorescent protein (GFP) vector plus empty pBin61 (lane 2) was used as a control. Noninfiltrated (NI) leaves were included in the analysis (lane 1). A GFP probe was used to detect the levels of GFP mRNA (upper panel), a GF probe to detect primary siRNAs (middle panel), and a P probe to detect secondary siRNAs (lower panel). RA data were calculated relative to GFP mRNA or siRNA accumulation in plants infiltrated with the GFP vector plus empty pBin61, which was arbitrarily set to 1. (c) Western blot analysis of total proteins from infiltrated leaves using anti-GFP monoclonal antibodies for detection of GFP protein. Ponceau S staining of the large subunit of RuBisCO protein was used as loading control. RA data were calculated relative to GFP accumulation in plants infiltrated with the GFP vector plus empty pBin61, which was arbitrarily set to 1. M: prestained protein marker. (d) GFP fluorescence from three assays was quantified by fluorescence spectrometry. Fluorescence measurement of each treatment was normalized to GFP plus GFFG and pBin61. The average amount is shown with standard deviations as error bars. Asterisks indicate significant differences between treatments (***$p < .001$) [Colour figure can be viewed at wileyonlinelibrary. com]

that are directly produced through hairpin processing by the plant Dicer-like (DCL) proteins were detected by northern blot using a "GF" probe. Relative abundance (RA) data were calculated relative

to GF siRNA accumulation in *N. benthamiana* plants agroinfiltrated with GFFG plus the empty vector pBin61, which was arbitrarily set to 1.

FIGURE 3 Evaluation of P0^{PL-Ar} protein mechanism through mutations in the F-box-like motif. (a) Alignment of the F-box-like motif of the P0 protein of different PLRV isolates: Argentinian (in red), European (GenBank: Y07496), Australian (GenBank: D13953.1), Peruvian (GenBank: KU586454.1), Indian (GenBank: JQ420903.1), North American (GenBank: KP090166.1), and Inner Mongolian (GenBank: KC456052). The red box indicates the imperfect F-box motif (positions 59 to 77) and the green box indicates the consensus F-box motif (positions 76 to 95). The conserved positions of the F-box motif are highlighted in black and the WG residues in red. The amino acid changes in the mutated versions of P0^{PL-Ar} protein are represented by underlined and bold lowercase letters. (b) *Nicotiana benthamiana* line 16c leaves were coinfiltrated with a mixture of *Agrobacterium tumefaciens* cultures harbouring a sense green fluorescent protein (GFP) inducer plus: pBin61 empty vector as a negative control (panel B and G), untagged version of P0^{PL-Ar} (panel C and H) as a positive control, c-Myc tagged version of P0^{PL-Ar} (panel C, G, and I), P0$^{PL-Ar-LP(76-77)AA}$ (panel E, G ,and J), and P0$^{PL-Ar-WG(87-88)AA}$ (panel E, G, and K). Noninfiltrated (NI) 16c plants (panel A) were used as a control. Panels H, I, J, and K are a magnification of panels C, D, E, and F, respectively, and arrows indicate the red halo bordering the infiltration patch. Photographs were taken under UV light 5 days postinfiltration (dpi). (c) GFP fluorescence from three assays was quantified by fluorescence spectrometry and normalized to GFP plus pBin61 empty vector. The average amount is shown with standard deviations as error bars. Asterisks indicate significant differences between treatments (*.001 < p < .01). (d) Systemic RNA silencing suppression assay. *N. benthamiana* 16c plants were infiltrated with mixtures harbouring GFP plus: pBin61 empty vector as a negative control (panel B), untagged version of P0^{PL-Ar} (panel C) as a positive control of systemic silencing, c-Myc-tagged version of P0^{PL-Ar} (panel D), and P0^{PL-Ar} mutants proteins P0$^{PL-Ar-LP(76-77)AA}$ and P0$^{PL-Ar-WG(87-88)AA}$ (panels E and F). NI 16c plants (panel A) were used as a control. Photographs of whole plants were taken under UV light 15 dpi. The proportion of plants with the phenotype shown in each panel is indicated. (e) Northern blot analysis of total RNA extracted from *N. benthamiana* 16c leaves 5 dpi infiltrated with a mixture of *A. tumefaciens* cultures harbouring a sense GFP inducer plus: pBin61 empty vector (lane 2), untagged version of P0^{PL-Ar} (lane 3), c-Myc-tagged version of P0^{PL-Ar} (lane 4), P0$^{PL-Ar-LP(76-77)AA}$ mutant (lane 5), or P0$^{PL-Ar-WG(87-88)AA}$ mutant (lane 6). NI leaves were included in the analysis (lane 1). A GFP probe was used to detect the levels of GFP mRNA and siRNA. Ethidium bromide-stained rRNA or low-molecular-weight (LMW) RNA were used as loading control. Relative abundance (RA) data were calculated relative to GFP plus pBin61 mRNA or siRNA accumulation, which was set arbitrarily to 1 [Colour figure can be viewed at wileyonlinelibrary.com]

At 5 dpi, primary siRNA accumulated in the absence of suppressor (Figure 2a, lane 1) or in presence of P0^{Tu} or P0^{CL} proteins (lanes 2 and 3). In contrast, patches agroinfiltrated with P0^{PL-Ar}, P0^{PL-NL}, and P38^{TCV} displayed a strong reduction of siRNA accumulation (Figure 2a, lanes 4, 5, and 6). Nevertheless, in contrast with P38^{TCV} (Figure 2a arrow), no accumulation of higher molecular weight material was detectable in P0^{PL-Ar} or in P0^{PL-NL} lanes in any of the assays performed. These results suggest that both P0^{PL-Ar} and P0^{PL-NL} act in a very early step of the silencing pathway suppressing hairpin-induced silencing, although this inhibition would be mechanistically different from P38^{TCV}-mediated silencing suppression.

During plant defence against viruses, a very important step in PTGS is the signal amplification through the action of different host-encoded RNA-dependent RNA polymerases (RDR) (Csorba et al., 2015). Because a small quantity of primary siRNA was observed with P0^{PL-Ar} (Figure 2a, lane 5), we examined whether P0^{PL-Ar} could also affect the production of secondary siRNAs. The agroinfiltration assays were performed in the presence of a construct expressing the complete GFP gene (sGFP). The secondary GFP siRNAs derived from the RNA-dependent RNA polymerase 6 (RDR6)-directed amplification were visualized by northern blots with a "P" probe that targets a GFP gene region outside of the GFFG hairpin (Bortolamiol et al., 2007).

At 5 dpi, patches infiltrated with P0^{PL-Ar}, P0^{PL-NL}, P0^{Tu}, and P0^{CL} displayed different intensities of green fluorescence, registered under UV light (Figure S1). Quantification of GFP fluorescence by spectrometry, which was consistent with GFP mRNA and protein levels (Figure 2b,c), confirmed visual observations and demonstrated that the observed differences between the suppressors analysed were significant (Figure 2d). As observed in *Agrobacterium*-infiltrated *N. benthamiana* 16c plants, both P0^{PL-NL} and P0^{PL-Ar} proteins triggered a cell death phenotype in the agroinfiltration area of

N. benthamiana leaves that was visible to the naked eye at 3 dpi (data not shown).

In accordance with previous results, primary siRNAs (detected with a "GF" probe) decreased drastically in plants agroinfiltrated with either of PLRV P0 isolates with respect to control silenced plants (Figure 2b, lanes 6 and 7 vs. 3) and plants inoculated with the other tested polerovirus VSRs (Figure 2b, lanes 4 and 5). In addition, secondary siRNAs (visualized using a "P" probe) were undetectable when GFP plus GFFG were coexpressed with P0^{PL} proteins. Taken together these results demonstrated that P0^{PL-Ar} and P0^{PL-NL} affect primary siRNA accumulation and, as well as P0^{Tu} and P0^{CL}, inhibit the formation of secondary siRNA. This suggests that the targeted step resides at the level of DCL action in the RNA silencing pathway.

3.3 | LP (L76/P77) and WG (W87/G88) in the F-box-like motif of P0^{PL-Ar} are required for suppression of RNA silencing

By comparing the functionality of two partially overlapping F-box like motifs in P0^{PL-IM}, Zhuo et al. (2014) demonstrated that the critical motif for its suppressor activity is between amino acids leucine 76 (L76) and proline 95 (P95). Moreover, these researchers revealed that residues tryptophan 87 and glycine 88 (W87/G88), within the P0^{PL-IM} F-box-like motif, which are absent from other poleroviral P0 sequences, are also critical for P0^{PL-IM} suppressor activity.

In order to analyse the importance of the region between amino acids L76 and P95 in the F-box like motif as well as amino acids W87 and G88 in the silencing suppressor activity of P0^{PL-Ar}, we generated different mutant proteins (Figure 3a). The amino acids L76 and P77 were replaced by alanine (A) to obtain the mutated protein P0$^{PL-Ar-LP(76-77)AA}$. In addition, the mutant protein P0$^{PL-Ar-WG(87-88)AA}$ had residues W87 and
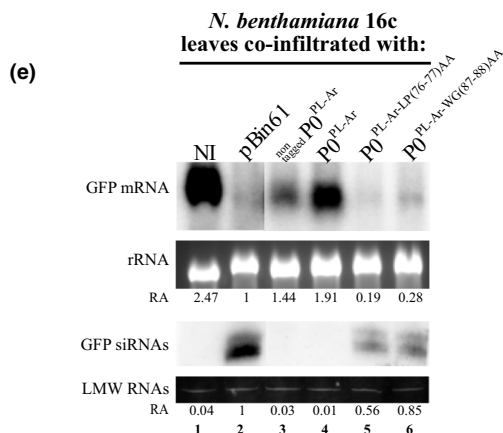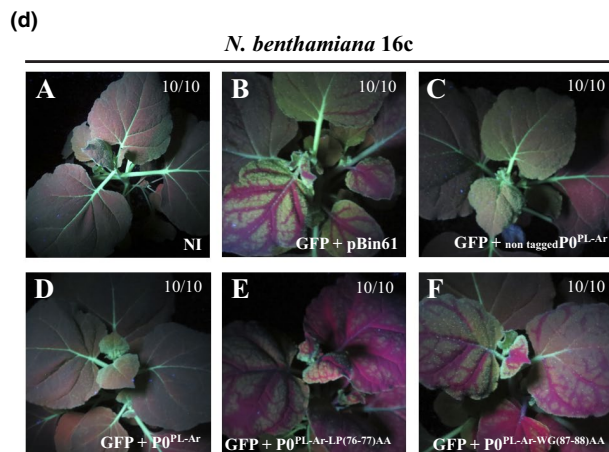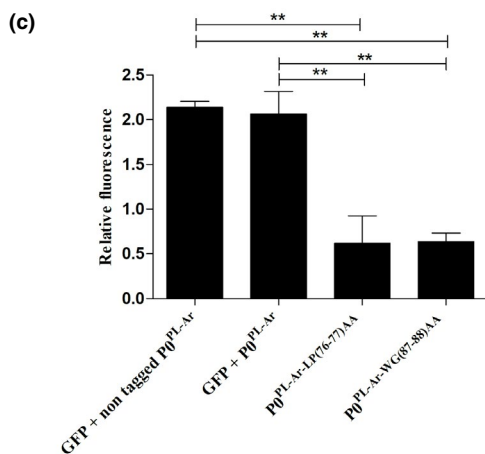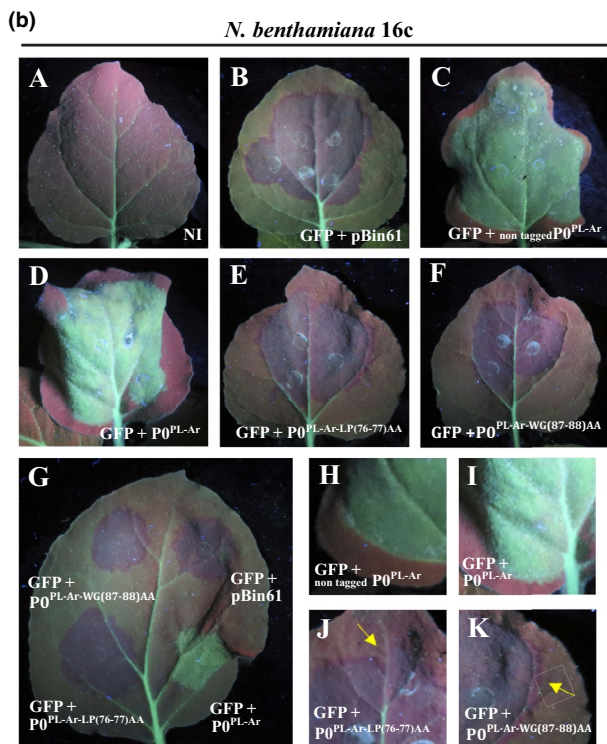
(a)


```
P0^PL-Ar (KY85683)         59 -LPLLNCKRGRISTSGLQLPRHLHYECLEWGLLCGTHP- 95
P0^PL-NL (Y07496)          59 -LPLLNCKRGRISTSGLQLPRHLHYECLEWGLLCGTHP- 95
P0^PL-Australian (D13953.1) 59 -LPLLNCKRGRISTSGLQLPRHLHYECLEWGLLCGTHP- 95
P0^PL-Peruvian (KU586454.1) 59 -LPLLNCKRGRISTSGLQLPRHLHYECLEWGLLCGTHP- 95
P0^PL-Indian (JQ420903.1)   59 -LPLLNCKRGRISTSGLQLPRHLHYECLEWGLLCGTHP- 95
P0^PL-USA (KP090166.1)     59 -LPLLNCKRGRISTSGLQLPRHLHYECLEWGLLCGTHP- 95
P0^PL-IM (KC456052)        59 -LPLLNCKRGRISTSGLQLPRHLHYECLEWGLLCGTHP- 95

P0^PL-Ar-LP(76-77)AA       59 -LPLLNCKRGRISTSGLQaaRHLHYECLEWGLLCGTHP- 95
P0^PL-Ar-WG(87-88)AA       59 -LPLLNCKRGRISTSGLQLPRHLHYECLEaaLLCGTHP- 95
```

(b)

N. benthamiana 16c

(c)

(d)

N. benthamiana 16c

(e)

N. benthamiana 16c
leaves co-infiltrated with:

	NI	pBin61	non tagged P0^PL-Ar	P0^PL-Ar	P0^PL-Ar-LP(76-77)AA	P0^PL-Ar-WG(87-88)AA
GFP mRNA						
rRNA						
RA	2.47	1	1.44	1.91	0.19	0.28
GFP siRNAs						
LMW RNAs						
RA	0.04	1	0.03	0.01	0.56	0.85
	1	2	3	4	5	6

G88 also substituted by alanine. In both cases, a c-Myc tag was fused to the carboxy-terminus of their coding sequences.

N. benthamiana 16c leaves were agroinfiltrated with a sense GFP inducer plus P0^PL-Ar or with either F-box mutant P0 proteins. c-Myc-tagged P0^PL-Ar was used as a control to discard any possible effect of c-Myc on P0 activity and pBin61 empty vector was used as a negative control. Although P0^PL-Ar c-Myc-tagged version showed higher GFP fluorescence and mRNA level than the untagged version, these differences were not significant (Figure 3c). GFP fluorescence was undetectable in patches infiltrated with P0^PL-Ar mutants or pBin61 empty vector at 5 dpi (Figure 3b), which was confirmed by GFP fluorescence quantification (Figure 3c). In contrast to P0^PL-Ar, leaves infiltrated with P0^PL-Ar-LP(76-77)AA and P0^PL-Ar-WG(87-88)AA displayed a red halo around the infiltrated patch at 5 dpi, which intensified over time (Figure 3b, panels E, F, J, and K). Additionally, neither of the mutant proteins developed the cell death phenotype triggered by P0^PL-Ar

FIGURE 4 Evaluation of silencing suppression triggered by an inverted-repeat sequence by P0^{PL-Ar} mutant proteins. (a) Leaves of *Nicotiana benthamiana* were infiltrated with a mixture of *Agrobacterium tumefaciens* containing a double-stranded RNA inducer "GFFG" plus either pBin61 empty vector (lane 1), P0^{Tu} (lane 2), P0^{CL} (lane 3), untagged version of P0^{PL-Ar} (lane 4), c-Myc-tagged version of P0^{PL-Ar} (lane 5), P0$^{PL-Ar-LP(76-77)AA}$ (lane 6), P0$^{PL-Ar-WG(87-88)AA}$ (lane 7), or P38^{TCV} as a negative control (lane 8). Total RNA was extracted and analysed for the presence of GF small RNA with a GF probe by northern blot. Ethidium bromide-stained low-molecular-weight (LMW) RNAs were used as loading control. Relative abundance (RA) data were calculated relative to GF siRNA accumulation in *N. benthamiana* plants agroinfiltrated with GFFG plus the empty vector pBin61, which was arbitrarily set to 1. The arrow indicates high-molecular-weight dsRNA. (b) *N. benthamiana* leaves were coinfiltrated with a mixture of *A. tumefaciens* containing GFP and GFFG plus either pBin61 (panel C), untagged version of P0^{PL-Ar} (panel D), c-Myc tagged version of P0^{PL-Ar} (panel E), P0$^{PL-Ar-LP(76-77)AA}$ (panel F) or P0$^{PL-Ar-WG(87-88)AA}$ (panel G). GFP vector plus pBin61 (panel B) was used as a control. Noninfiltrated (NI) leaves were included in the analysis (panel A). Photographs were taken under UV light 5 dpi. (c) Total RNA extracted from *N. benthamiana* leaves patches (5 dpi) infiltrated with a mixture of *A. tumefaciens* cultures harbouring sense GFP and dsRNA inducer GFFG plus either pBin61 empty vector (lane 3), P0^{Tu} (lane 4), P0^{CL} (lane 5), untagged version of P0^{PL-Ar} (lane 6), c-Myc-tagged version of P0^{PL-Ar} (lane 7), P0$^{PL-Ar-LP(76-77)AA}$ (lane 8), or P0$^{PL-Ar-WG(87-88)AA}$ (lane 9) were analysed by northern blot. GFP vector plus pBin61 (lane 2) was used as a control. NI leaves were included in the analysis (lane 1). RNAs were detected with a specific probe to analyse GFP mRNA, GFP primary siRNAs (upper panel) or P secondary siRNAs (lower panel). Ethidium bromide-stained rRNA or low-molecular-weight (LMW) RNAs were used as loading control. Relative abundance (RA) data was calculated relative to GFP plus GFFG and pBin61 mRNA or siRNA accumulation, which was arbitrarily set to 1. (d) GFP fluorescence from three assays was quantified by fluorescence spectrometry. Fluorescence measurement of each treatment was normalized to GFP plus GFFG and pBin61. The average amount is shown with standard deviations as error bars. Asterisks indicate significant differences between treatments (*.01 < p < .05) [Colour figure can be viewed at wileyonlinelibrary.com]

(Figure S2). However, at 15 dpi, while plants agroinfiltrated with P0^{PL-Ar} exhibited a systemic silencing suppression phenotype, plants agroinfiltrated with P0$^{PL-Ar-LP(76-77)AA}$ or P0$^{PL-Ar-WG(87-88)AA}$ showed GFP silencing in upper leaves, similar to plants agroinfiltrated with pBin61 empty vector (Figure 3d).

Northern blot revealed a decrease in GFP mRNA accumulation in agroinfiltrated patches with either F-box mutant in comparison to accumulation with P0^{PL-Ar} (Figure 3e, lanes 3, 4, 5, and 6). Conversely, the same samples displayed an increase in GFP siRNA production relative to samples from leaves agroinfiltrated with P0^{PL-Ar} (Figure 3e, lanes 3, 4, 5, and 6).

Taken together, these results indicate that the mutations generated in P0$^{PL-Ar-LP(76-77)AA}$ and P0$^{PL-Ar-WG(87-88)AA}$ abolish the suppressor activity of P0^{PL-Ar} protein, both locally and systemically. Thus, positions L76/P77 and W87/G88 in the F-box motif are fundamental for P0^{PL-Ar} functionality as an RNA silencing suppressor.

Moreover, to investigate whether mutations in residues L76/P77 and W87/G88 differentially affect primary and secondary siRNA generation, we subsequently infiltrated *N. benthamiana* leaves with a mixture of *A. tumefaciens* containing a dsRNA inducer "GFFG" plus either pBin61 empty vector, P0^{Tu}, P0^{CL}, untagged version of P0^{PL-Ar}, c-Myc-tagged version of P0^{PL-Ar}, P0$^{PL-Ar-LP(76-77)AA}$, P0$^{PL-Ar-WG(87-88)AA}$, or P38^{TCV} as a negative control. Northern blot analyses with a GF probe revealed that at 5 dpi, unlike results with P0^{PL-Ar}, hairpin-derived siRNAs were detectable in both P0$^{PL-Ar-LP(76-77)AA}$ and P0$^{PL-Ar-WG(87-88)AA}$ (Figure 4a, lanes 6 and 7). Therefore, these results suggest that mutations at residues L76/P77 and W87/G88 of P0^{PL-Ar} affect the ability of P0^{PL-Ar} to suppress GF hairpin-induced silencing.
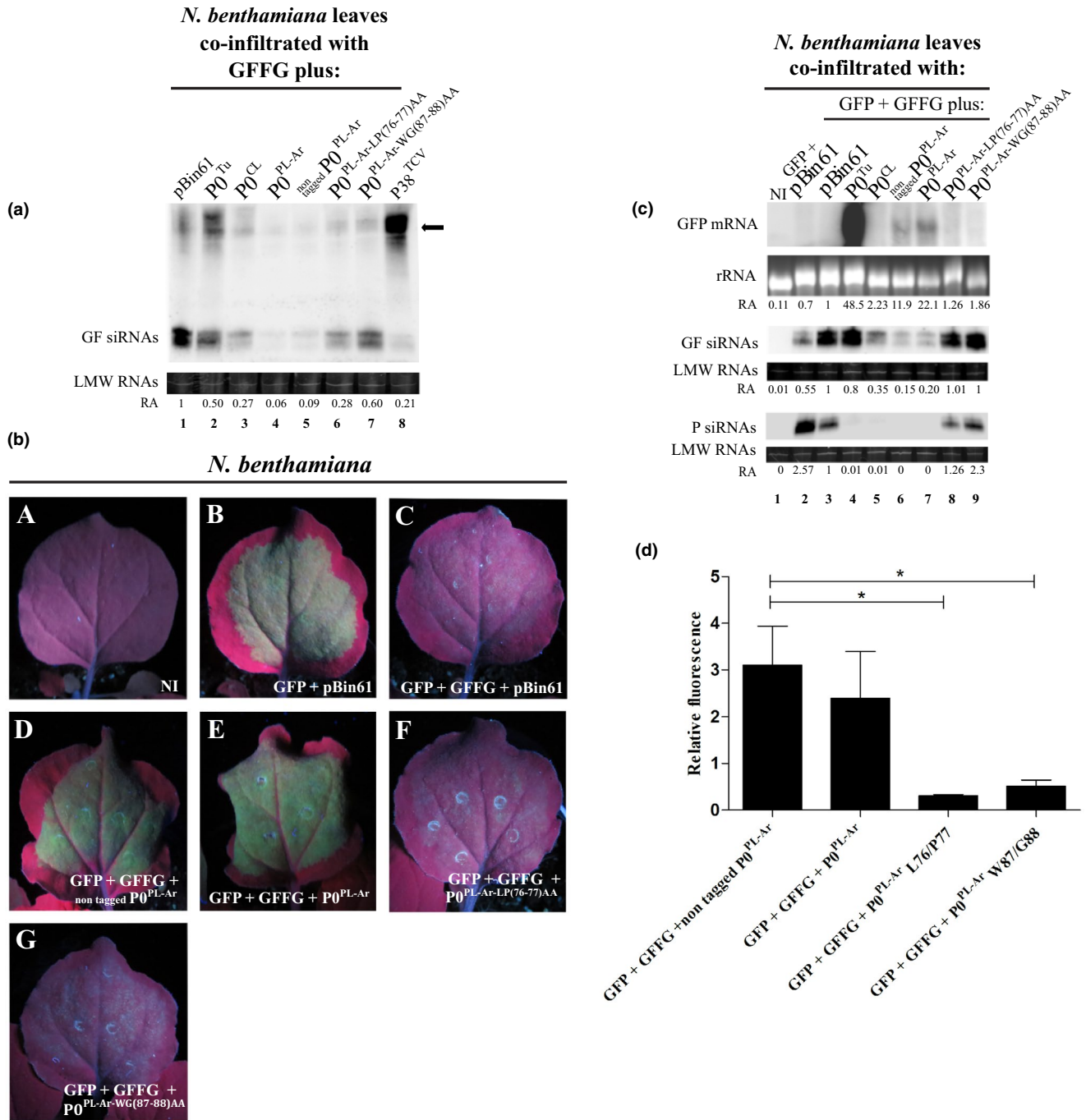
Considering the above results and with the objective to evaluate the effect of P0^{PL-Ar} mutants on secondary siRNA production, we repeated the experiment in the presence of a complete copy of GFP. P0^{PL-Ar}, P0^{Tu}, and P0^{CL} proteins were used as controls. As in the *N. benthamiana* 16c transient assay (Figure 3b), patches infiltrated with P0$^{PL-Ar-LP(76-77)AA}$ or P0$^{PL-Ar-WG(87-88)AA}$ remained red, similar to control plants infiltrated with

the empty vector (Figure 4b, panels C, F, and G). Additionally, neither of the mutant proteins developed the cell death phenotype triggered by P0^{PL-Ar} (data not shown). The strong decline of GFP fluorescence was confirmed by spectrometry quantification, with significant differences (Figure 4d). Accordingly, no GFP mRNA accumulated in patches of plants agroinfiltrated with P0$^{PL-Ar-LP(76-77)AA}$ or P0$^{PL-Ar-WG(87-88)AA}$ (Figure 4c, lanes 8 and 9), in contrast to the evident accumulation in patches of plants agroinfiltrated with P0^{PL-Ar} (Figure 4c, lanes 6 and 7). As found previously, primary siRNAs accumulated in the presence of P0^{PL-Ar} (Figure 4c, lanes 6 and 7) were barely detectable; however, in the presence of P0$^{PL-Ar-LP(76-77)AA}$ or P0$^{PL-Ar-WG(87-88)AA}$, they were similar to those observed in the presence of P0^{Tu} or pBin61 control (Figure 4c, lanes 3 and 4). In contrast, when a "P" probe was used to detect secondary siRNA production, a similar level was detected with the F-box mutants (Figure 4c, lanes 8 and 9) and with the empty vector control lane (Figure 4c, lanes 2 and 3).

Altogether, the residues L76, P77, W87, and G88 present in the F-box like motif are fundamental for P0^{PL-Ar} functionality as an RNA silencing suppressor. In addition, mutations in positions L76/P77 and W87/G88 affect P0^{PL-Ar} at the same step in the silencing pathway, because both mutants are unable to impede siRNA accumulation.

3.4 | Wild-type P0^{PL-Ar} interacts with *S. tuberosum* SKP1 (StSKP1)

The interaction of PLRV P0 protein with SKP1-like proteins has only been studied for two PLRV isolates with differing results. The European PLRV P0 protein interacts weakly with *N. benthamiana* NbSKP1 but not with *A. thaliana* ASK1 and ASK2 (Pazhouhandeh, 2007). However, P0 protein encoded by the Inner Mongolian PLRV does not interact with NbSKP1 (Zhuo et al., 2014). Considering that the F-box motif is required for P0^{PL-Ar} silencing suppression activity, we analysed the interaction of this protein with ASK1, ASK2, NbSKP1 and with the orthologue in *S. tuberosum* (StSKP1) using a Y2H system.

(a)

N. benthamiana leaves co-infiltrated with GFFG plus:

Lanes: pBin61, P0^{Tu}, P0^{CL}, P0^{PL-Ar}, non tagged P0^{PL-Ar}, P0$^{PL-Ar-LP(76-77)AA}$, P0$^{PL-Ar-WG(87-88)AA}$, P38 TCV

GF siRNAs

LMW RNAs

RA: 1 0.50 0.27 0.06 0.09 0.28 0.60 0.21

1 2 3 4 5 6 7 8

(b)

N. benthamiana

A — NI
B — GFP + pBin61
C — GFP + GFFG + pBin61
D — GFP + GFFG + non tagged P0^{PL-Ar}
E — GFP + GFFG + P0^{PL-Ar}
F — GFP + GFFG + P0$^{PL-Ar-LP(76-77)AA}$
G — GFP + GFFG + P0$^{PL-Ar-WG(87-88)AA}$

(c)

N. benthamiana leaves co-infiltrated with:

GFP + GFFG plus:

Lanes: NI, GFP + pBin61, pBin61, P0^{Tu}, P0^{CL}, non tagged P0^{PL-Ar}, P0^{PL-Ar}, P0$^{PL-Ar-LP(76-77)AA}$, P0$^{PL-Ar-WG(87-88)AA}$

GFP mRNA
rRNA
RA: 0.11 0.7 1 48.5 2.23 11.9 22.1 1.26 1.86

GF siRNAs
LMW RNAs
RA: 0.01 0.55 1 0.8 0.35 0.15 0.20 1.01 1

P siRNAs
LMW RNAs
RA: 0 2.57 1 0.01 0.01 0 0 1.26 2.3

1 2 3 4 5 6 7 8 9

(d)

Relative fluorescence

Categories: GFP + GFFG + non tagged P0^{PL-Ar}, GFP + GFFG + P0^{PL-Ar}, GFP + GFFG + P0^{PL-Ar} L76/P77, GFP + GFFG + P0^{PL-Ar} W87/G88

ORFs of P0^{PL-Ar}, P0$^{PL-Ar-LP(76-77)AA}$, P0$^{PL-Ar-WG(87-88)AA}$, and of the different SKP1-like proteins were amplified and cloned into Y2H vectors pGADT7 and pGBKT7, respectively. Independent colonies cotransformed with all the combinations were replicate-streaked on double transformant control media (−LW) or stringent selective media (−LWHA). As expected, all double-transformed yeast cells were able to grow on −LW medium (Figure 5a). P0^{PL-Ar} was able to interact with StSKP1 as well as with ASK1 and ASK2 but failed to interact with NbSKP at either 21 or 28°C (Figure 5a). On the other hand, the F-box silencing-suppression-defective mutants, P0$^{PL-Ar-LP(76-77)AA}$ and P0$^{PL-Ar-WG(87-88)AA}$, failed to interact with potato protein StSKP1, although both interacted with *A. thaliana* orthologues ASK1 and ASK2 (Figure 5a).
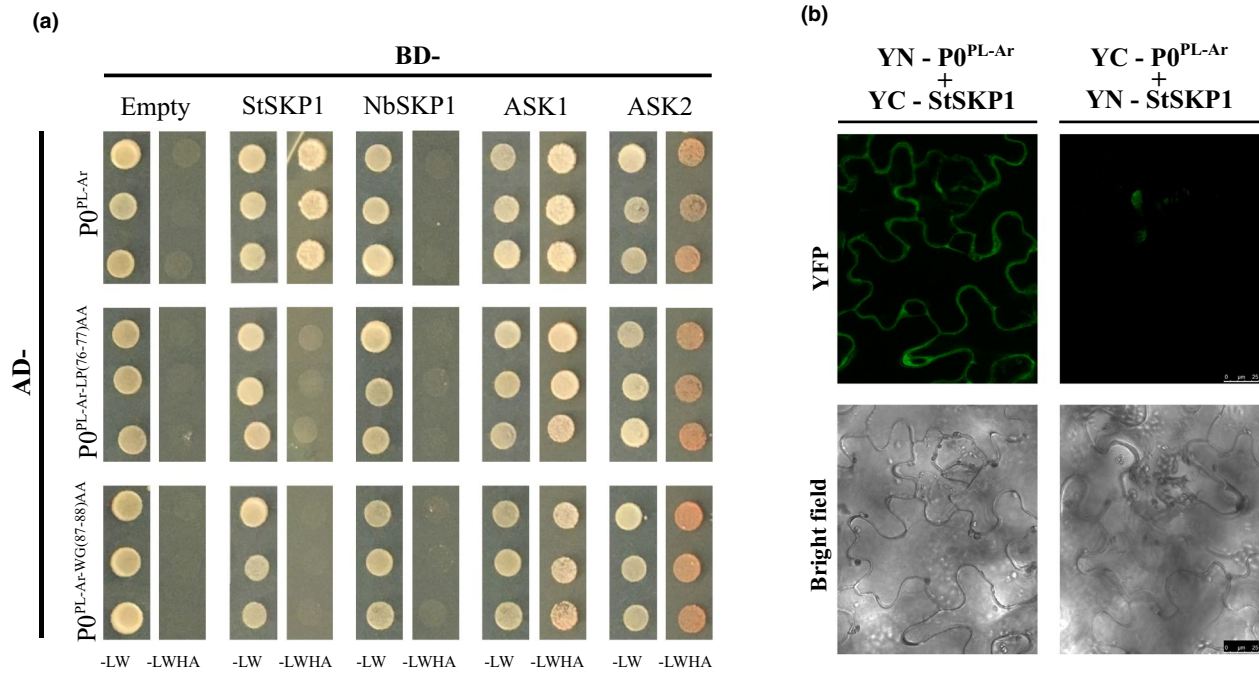
FIGURE 5 Interaction assays between P0^{PL-Ar} and SKP1 proteins. (a) Interaction between P0^{PL-Ar} and its mutants with NbSKP1; ASK1, ASK2, and StSKP1 proteins were investigated using yeast two-hybrid system. Yeast cells were cotransformed with empty pGBK vector as a negative control, pGBK:NbSKP1, pGBK:ASK1, pGBK:ASK2, or pGBK:StSKP1 and one of the following constructs: pGAD:P0^{PL-Ar}, pGAD:P0$^{PL-Ar-LP(76-77)AA}$, pGAD:P0$^{PL-Ar-WG(87-88)AA}$. As a control of possible false positives, yeasts were transformed with pGBKT7-P0^{PL-Ar} and the empty pGAD vector or with pGAD-P0^{PL-Ar} and pGBK empty. As a positive control of the interaction, yeasts were transformed with the vectors pGBK-P0^{Tu} and pGAD-ASK1, an interaction described by Pazhouhandeh et al. (2006). Cells grew on a medium deprived of leucine and tryptophane (−LW) as doubled transformed control and on selective media (deprived of leucine, tryptophan, histidine, and adenine, [−LWHA]) to evaluate the interaction. Each combination is shown in triplicate. (b) Bimolecular fluorescence complementation experiments with transiently expressed P0$^{PLRV-Ar}$ and StSKP1 fusion proteins. Tobacco leaf epidermal cells were co-agroinfiltrated for expression of the indicated combinations: VYNER(YN)-P0^{PL-Ar} plus VYCER(YC)-StSKP1 and VYCER(YC)-P0^{PL-Ar} plus VINER(YN)-StSKP1. The results are representative of three independent experiments. Scale bar = 25 μm [Colour figure can be viewed at wileyonlinelibrary.com]

To confirm the in planta interaction between P0^{PL-Ar} and StSKP1, BiFC assays were performed. Leaves of *N. benthamiana* were coinfiltrated with the complete coding sequences of P0^{PL-Ar} or StSKP1 fused to the C-terminal (VYCER) or the N-terminus fragment of Venus (VYNER) (hereinafter referred to as YC or YN, respectively).

The BiFC assays showed fluorescence signal in *N. benthamiana* epidermal cells coexpressing P0^{PL-Ar} and StSKP1 when the N-terminal of Venus (YN) was fused to the amino-terminus of P0^{PL-Ar} and the C-terminal of Venus (YC) was fused to the amino-terminus of StSKP1 (Figure 5b). In conclusion, these results demonstrated that P0^{PL-Ar} interacts with StSKP1 in either yeast or plants.

Therefore, our data showed that the interaction of P0^{PL-Ar} with the SKP component of the SCF ubiquitin ligase complex is conserved in *S. tuberosum* and in a non-natural host such as *A. thaliana*. However, based on the results obtained, we conclude that some differences could exist between both interactions, because the amino acids L76/P77 and W87/G88 in the F-box motif are essential only for the interaction between P0^{PL-Ar} and StSKP1.

3.5 | P0PL-Ar silencing activity and interaction with StSKP1 are correlated with reduced AGO1 accumulation

Recently, different groups have demonstrated that PLRV P0 proteins from Australian and Inner Mongolian isolates destabilize ARGONAUTE 1 (AGO1), although, at least P0^{PL-IM} does not interact with SKP1 (Fusaro et al., 2012; Zhuo et al., 2014). To test whether P0^{PL-Ar} induces AGO1 destabilization, we subsequently performed agroinfiltration assays developed by Baumberger et al. (2007). An N-terminal GFP-tagged version of *A. thaliana* AGO1 (Derrien et al., 2012) was transiently expressed in *N. benthamiana* leaves by coinfiltration with the 4 × Myc-tagged P0^{PL-Ar} or the F-box mutant versions. Tomato bushy stunt virus (TBSV) P19 (a VSR) was also coinfiltrated to avoid RNA silencing of the exogenous transcripts and to ensure its correct expression during the transient expression assay.

At 3 dpi, the protein extracts from the infiltrated patches were analysed by western blotting using anti-GFP to detect eGFP-AGO1 protein or anti-cMyc tag antibodies to detect P0 proteins. eGFP-AGO1 was detected in control infiltrated leaves (pBin61;

Figure 6, lane 2). Coexpression of eGFP-AGO1 with P0^{PL-Ar} or the silencing-suppression-defective mutant P0$^{PL-Ar-LP(76-77)AA}$ led to undetectable levels of eGFP-AGO1 signal, similar to the results with the P0 controls (Figure 6, lanes 3, 4, 5, 6, and 7). In contrast, no effect on eGFP-AGO1 accumulation was detectable with the other silencing-suppression-defective mutant (P0$^{PL-Ar-WG(87-88)AA}$) (Figure 6, lane 8), even though the mutant protein accumulated to normal levels as revealed by western blot with the anti-cMyc antibody (Figure 6, lane 8).

These results show that P0^{PL-Ar} affects AGO1 accumulation greatly reducing its levels. Furthermore, residues W87/G88 in the F-box motif are essential for this function, while mutations in residues L76/P77 seem not to affect P0^{PL-Ar} capacity to destabilize AGO1.

4 | DISCUSSION

In this study, we characterized the RNA suppressor activity of P0 protein from the Argentinian isolate of PLRV (P0^{PL-Ar}). Transient expression assays in *N. benthamiana* line 16c demonstrated that P0^{PL-Ar} interferes with local and systemic RNA silencing.

Several VSRs have been reported to exert their action during early steps of the silencing pathway (Csorba et al., 2015). Among

FIGURE 6 Analysis of AGO1 protein accumulation. *Nicotiana benthamiana* leaves were infiltrated with a mixture of *Agrobacterium tumefaciens* cells harbouring constructs expressing green fluorescent protein (GFP)-tagged version of *Arabidopsis thaliana* ARGONAUTE 1 (eGFP-AGO1) and the tomato bushy stunt virus viral suppressor of RNA silencing, P19 plus either empty pBin61 vector (lane 2) used as a negative control, P0^{Tu} (lane 3), P0^{CL} (lane 4), both as positive controls, untagged version of P0^{PL-Ar} (lane 5), c-Myc-tagged version of P0^{PL-Ar} (lane 6), P0$^{PL-Ar-LP(76-77)AA}$ (lane 7), or P0$^{PL-Ar-WG(87-88)AA}$ (lane 8). 4 × Myc-tagged P0 proteins of turnip yellows virus (P0^{Tu}) and cotton leafroll dwarf virus (P0^{CL}) were used as positive controls for the destabilization of AtAGO1. Total proteins were extracted from infiltrated leaves 3 days postinfiltration (dpi) and analysed by western blot using anti-GFP polyclonal antibody to detect eGFP-AGO1 protein and anti-c-Myc monoclonal antibody to detect P0 proteins. Ponceau S staining of the large subunit of RuBisCO protein was used as loading control. M: prestained protein marker [Colour figure can be viewed at wileyonlinelibrary.com]

them, TCV P38 and TBSV P19 have been extensively studied. Iki et al. (2017) demonstrated that P38^{TCV} interacts physically with long dsRNA, in a size-dependent manner, and that this binding is required for the inhibition of its processing. Alternatively, P19^{TBSV} interacts physically and sequesters siRNA duplexes, preventing RISC assembly (Lakatos et al., 2006; Schuck et al., 2013). Remarkably, our results revealed that in an IR-PTGS assay, P0^{PL-Ar} impeded the accumulation of hairpin-derived siRNAs, similar to P38^{TCV} (Iki et al., 2017). However, these VSRs showed differences, because higher molecular weight dsRNAs did not accumulate in the presence of P0^{PL-Ar}. Mérai et al. (2005) observed similar results for P14 protein of the pothos latent virus (PoLV), a tombusvirus close relative. These authors suggested that during PoLV infection, P14 would inhibit host defence systemic silencing by sequestration or deceleration of siRNA generation, thus allowing PoLV to colonize the plant. Based on our results, we cannot be sure whether P0^{PL-Ar} would act like P38 or P19. However, considering that P0^{PL-Ar} is a suppressor of systemic silencing, we suggest a similar scenario to that of P14.

The fact that P0^{PL-Ar} interferes in a very early step of the silencing pathway differs from previously reported data for other polerovirus P0 proteins, which act downstream of DCL-mediated cleavage (Bortolamiol et al., 2007; Fusaro et al., 2012; Delfosse et al., 2014; Almasi et al., 2015; Li et al., 2019). To our knowledge, this is the first report of a poleroviral and PLRV P0 protein that prevents hairpin-derived siRNA accumulation.

This study also showed that P0^{PL-Ar} prevents the accumulation of secondary siRNAs, which depends on cellular AGO1 and RDR6 proteins. These results agree with those reported for P0 of the Australian isolate of PLRV (Fusaro et al., 2012) and for P0 proteins of other poleroviruses (Bortolamiol et al., 2007; Delfosse et al., 2014; Almasi et al., 2015).

The RNA silencing suppressor activity of P0 proteins of TuYV, cucurbit aphid-borne yellows virus (CABYV), CLRDV, and brassica yellows virus (BrYV) depends on the presence of a conserved F-box like motif (LPxx (L/I) x10-13P) that mediates the interaction with SKP1 and leads to ubiquitination and degradation of AGO. Mutations on LP residues deprive these proteins of their suppressor activity (Pazhouhandeh et al., 2006; Almasi et al., 2015; Agrofoglio et al., 2019; Li et al., 2019;). Zhuo et al. (2014) demonstrated that, although an Inner Mongolian PLRV isolate P0 protein has two F-box like motifs, only the motif located between positions 76 to 95, and not the imperfect one residing amongst amino acids 59 and 77, is functional in this protein. Indeed, mutations on residues L76 and P77 produced the loss of suppressor activity of P0^{PL-IM}. Similarly, Rashid et al. (2019) reported that L76F and W87R substitutions in the F-box-like motif of the P0 protein from a Canadian PLRV isolate as well as G139RRR substitution in the G139/W140/G141-like motif abolished P0's activity and PLRV systemic infection. Both F-box motifs identified in P0^{PL-IM} (Zhuo et al., 2014) are highly conserved in different PLRV isolates as well as in the Argentinian P0^{PL} protein.

The function of P0^{PL-Ar} was assessed by constructing P0 mutants with alanine substitutions in positions L76/P77 and W87/G88. These mutant proteins showed no suppressor functions, either
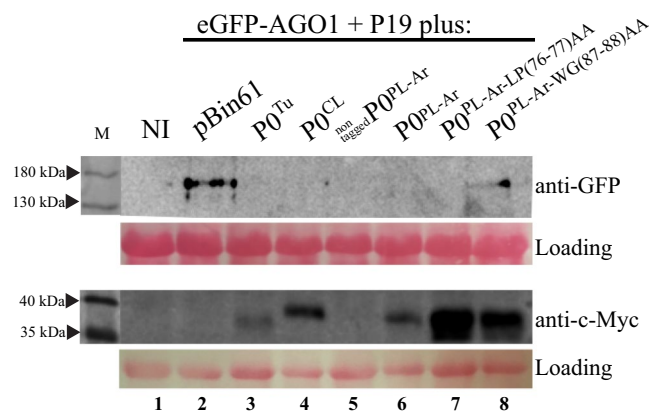
locally or systemically. In addition, neither of the mutants interfered with the production of primary siRNAs mediated by DCL enzymes, in a dsRNA-inducing hairpin assay. This result demonstrates that positions L76/P77 and W87/G88 of P0^{PL-Ar} are critical to impede primary siRNA accumulation. In the presence of either of the two P0^{PL-Ar} F-box mutants, the amplification process is established, and secondary siRNAs are generated. Furthermore, these results agree with the fact that these mutations abolished P0^{PL-Ar} suppression of systemic RNA silencing.

In the present study, we showed, for the first time, that P0^{PL-Ar} interacts with *S. tuberosum* (PLRV natural host) SKP1-like protein (StSKP1) both by Y2H and by BiFC in plants. In addition, we demonstrated that P0^{PL-Ar} interacts with *A. thaliana* ASK1 and ASK2 proteins, as shown for other members of the *Polerovirus* genus (Pazhouhandeh et al., 2006; Almasi et al., 2015; Agrofoglio et al., 2019). Interestingly, P0^{PL-Ar} failed to interact with *N. benthamiana* orthologue NbSKP1, despite sharing 94% amino acid sequence identity with StSKP1. These results agree with those of Zhuo et al. (2014) in studies with P0^{PL-IM}. However, by Y2H assays, Pazhouhandeh (2007) demonstrated that P0^{PL-NL} interacts, albeit weakly, with NbSKP1. Wang et al. (2015) reported a cell death phenotype in leaves of *Nicotiana glutinosa* (accessions TW59 and TW61) and *N. benthamiana* infected with PVX heterologous constructs expressing P0^{PL} or other poleroviral P0 proteins. These authors mutated TuYV's P0 F-box motif and this mutant was unable to elicit the cell death phenotype. Therefore, they suggested that the interaction between P0 proteins and E3 ubiquitin ligase complex is responsible for triggering cell death. Considering that P0^{PL-Ar}, unlike P0^{PL-Ar} mutant proteins, presents a severe necrosis in *N. benthamiana* (data not shown) and *N. benthamiana* 16c inoculated leaves, we propose that P0^{PL-Ar} could interact with an NbSKP1 paralogue, or with another intermediate protein capable of binding to NbSKP1, and that this interaction could be lost in the F-box mutants. Li et al. (2019) observed that P0^{BrYV} F-box mutants that are unable to interact with SKP are less or not detected in *N. benthamiana* leaves by western blot, and therefore proposed a novel model in which the P0^{BrYV}-SKP1 interaction is essential for P0^{BrYV} stability, preventing its degradation by host cells. Furthermore, this stability would assure efficient RNA silencing suppression. In contrast, western blot analyses with P0$^{PL-Ar-LP(76-77)AA}$ and P0$^{PL-Ar-WG(87-88)AA}$ showed equivalent protein accumulation to that of wild type P0^{PL-Ar}, indicating that for P0^{PL-Ar} F-box mutants the lack of RNA silencing suppression is not due to protein degradation. Therefore, we suggest that the conservation of P0^{PL-Ar} second F-box-like motif is essential for the interaction with its main host StSKP1 protein and to maintain its role as a VSR. In addition, although amino acid substitution within the F-box-like motif, L76/P77 and W87/G88, abolishes P0^{PL-Ar} capacity to interact with StSKP1, this substitution does not affect ASK1 and ASK2 interaction. A possible explanation is that mutations might cause conformational changes that affect differently P0^{PL-Ar} capacity to interact with SKP1 orthologues; alternatively, as Almasi et al. (2015) proposed for CYDV, P0^{PL-Ar}

first and imperfect F-box motif could be the one involved in ASK1 and ASK2 interactions.

Apart from poleroviral P0 proteins, several VSRs have been suggested to suppress RNA silencing by targeting AGO1 for degradation. Cucumber mosaic virus (CMV) 2b protein, for example, specifically inhibits the RISC complex through physically binding PAZ domains of the host AGO1/AGO4 proteins (Hamera et al., 2012). Recently, several researchers have demonstrated that the ipomoviral P1 suppressor and P38^{TCV} protein bind directly and specifically to AGO1 (Giner et al., 2010; Iki et al., 2017) and that this interaction affects RISC complex activity. The binding between these proteins and AGO1 would occur through their GW/WG motifs, imitating the GW/WG motif encoded by the host proteins needed for the assembly and/or performance of the RISC complex in several organisms (El-Shami et al., 2007). In the present study, both residues W87/G88, present in the P0^{PL-Ar} F-box-like motif, turned out to be critical for the protein suppressor function. We found that P0^{PL-Ar} reduced AGO1 protein accumulation to almost undetectable levels in accordance with previous reports, in which P0^{PL} from Australian and Inner Mongolian isolates destabilized the AGO1 protein (Fusaro et al., 2012; Zhuo et al., 2014). In this research, we demonstrated that only P0$^{PL-Ar-WG(87-88)AA}$ lost the ability to destabilize AGO1, whereas P0$^{PL-Ar-LP(76-77)AA}$ acted in the same way as the wild-type P0^{PL-Ar}. Nonetheless, no mutant protein was able to interfere with the primary production of siRNAs from dsRNA and therefore the mutations abolished P0 ability to suppress RNA silencing. These observations suggest that the WG motif in the second F-box-like motif of P0^{PL-Ar} has the typical characteristics of GW/WG motifs. As Zhuo et al. (2014) suggested, the location of W87/G88 within P0^{PL-Ar} F-box motif boundaries (76-LPRHLHYECLEWGLLCGTHP-95) is unusual for these poleroviral proteins and may affect P0^{PL-Ar} suppressor function by conferring interactions with other proteins or causing conformational changes in the protein.

In conclusion, this study contributes to the understanding of the different ways polerovirus P0 proteins function as silencing suppressors. Our results lead us to propose a model in which P0^{PL-Ar} exerts its action at more than one level of the RNA silencing pathway. P0^{PL-Ar} would act at a very early step by interfering with the generation of dsRNA-derived siRNA. On the other hand, through the WG motif in its F-box motif, P0^{PL-Ar} would act downstream of the RISC complex level by inducing AGO1 destabilization. Furthermore, P0^{PL-Ar} would act as an F-box protein, like P0 proteins of TuYV, CABYV, BrYV, and CLRDV (Baumberger et al., 2007; Bortolamiol et al., 2007; Csorba et al., 2010; Delfosse et al., 2014; Agrofoglio et al., 2019; Li et al., 2019). Indeed, P0^{PL-Ar} would interact with SKP proteins of the SCF complex through the conserved LP residues of the F-box motif and target proteins other than AGO1 (for example other ARGONAUTE proteins) for degradation.

Further studies are needed to unravel how P0^{PL-Ar} affects accumulation of dsRNA-derived siRNAs, addressing whether P0^{PL-Ar} interacts directly or indirectly with dsRNA, as well as to explore new cellular targets of P0^{PL-Ar} that would contribute to elucidating the mechanism of action of this silencing suppressor protein.

ACKNOWLEDGEMENTS

DATA AVAILABILITY STATEMENT

The data that support the findings of this study are available from the corresponding author upon reasonable request.

ORCID

Cecilia Vazquez Rovere https://orcid.org/0000-0002-5804-6197
Ana J. Distéfano https://orcid.org/0000-0002-9685-1103

REFERENCES

Agrofoglio, Y.C., Delfosse, V.C., Casse, M.F., Hopp, H.E., Bonacic Kresic, I. and Distéfano, A.J. (2019) P0 protein of cotton leafroll dwarf virus-atypical isolate is a weak RNA silencing suppressor and the avirulence determinant that breaks the cotton *Cbd* gene-based resistance. *Plant Pathology*, 68, 1059–1071.

Almasi, R., Miller, A.W. and Ziegler-Graff, V. (2015) Mild and severe cereal yellow dwarf viruses differ in silencing suppressor efficiency of the P0 protein. *Virus Research*, 208, 199–206.

Barrios Barón, M.P., Agrofoglio, Y.C., Delfosse, V.C., Nahirñak, V., Gonzalez de Urreta, M., Almasia, N.I. et al. (2017) First complete genome sequence of potato leafroll virus from Argentina. *Genome Announcements*, 5, 4–5.

Baumberger, N., Hsui, T.C., Lie, M., Havecker, E. and Baulcombe, D.C. (2007) The polerovirus silencing suppressor P0 targets ARGONAUTE proteins for degradation. *Current Biology*, 17, 1609–1614.

Bortolamiol, D., Pazhouhandeh, M., Marrocco, K., Genschik, P. and Ziegler-Graff, V. (2007) The polerovirus F-box protein P0 targets ARGONAUTE1 to suppress RNA silencing. *Current Biology*, 17, 1615–1621.

Chen, S., Jiang, G., Wu, J., Liu, Y., Qian, Y. and Zhou, X. (2016) Characterization of a novel polerovirus infecting maize in China. *Viruses*, 8, 120–136.

Csorba, T., Kontra, L. and Burgyán, J. (2015) Viral silencing suppressors: tools forged to fine-tune host–pathogen coexistence. *Virology*, 479, 85–103.

Csorba, T., Lózsa, R., Hutvágner, G. and Burgyán, J. (2010) Polerovirus protein P0 prevents the assembly of small RNA-containing RISC complexes and leads to degradation of ARGONAUTE1. *The Plant Journal*, 62, 463–472.

Delfosse, V.C., Agrofoglio, Y.C., Casse, M.F., Bonacic Kresic, I., Hopp, H.E., Ziegler-Graff, V. et al. (2014) The P0 protein encoded by cotton leafroll dwarf virus (CLRDV) inhibits local but not systemic RNA silencing. *Virus Research*, 180, 70–75.

Derrien, B., Baumberger, N., Schepetilnikov, M., Viotti, C., De Cillia, J., Ziegler-Graff, V. et al. (2012) Degradation of the antiviral component ARGONAUTE1 by the autophagy pathway. *Proceedings of the National Academy of Sciences of the United States of America*, 109, 15942–15946.

Ding, S.W. (2010) RNA-based antiviral immunity. *Nature Reviews Immunology*, 10, 632–644.

Domier, L.L. (2012) Family *Luteoviridae*. In: Carstens, E.B., Andrew, M.Q.K., Elliot, L. and Michael, J.A. (Eds.) *Virus Taxonomy: Ninth Report of the International Committee on Taxonomy of Viruses*. San Diego, CA: Elsevier Academic Press, pp. 193–210.

El-Shami, M., Pontier, D., Lahmy, S., Braun, L., Picart, C., Vega, D. et al. (2007) Reiterated WG/GW motifs form functionally and evolutionarily conserved ARGONAUTE-binding platforms in RNAi-related components. *Genes & Development*, 21, 2539–2544.

Fusaro, A.F., Corrêa, R.L., Nakasugi, K., Jackson, C., Kawchuk, L., Vaslin, M.F.S. et al. (2012) The *Enamovirus* P0 protein is a silencing suppressor which inhibits local and systemic RNA silencing through AGO1 degradation. *Virology*, 426, 178–187.

Gehl, C., Waadt, R., Kudla, J.R., Mendel, R. and Hä, R. (2009) New Gateway vectors for high throughput analyses of protein–protein interactions by bimolecular fluorescence complementation. *Molecular Plant*, 2, 1051–1058.

Giner, A., Lakatos, L., García-Chapa, M., López-Moya, J.J. and Burgyán, J. (2010) Viral protein inhibits RISC activity by ARGONAUTE binding through conserved WG/GW motifs. *PLoS Pathogens*, 6, e1000996.

Hamera, S., Song, X., Su, L., Chen, X. and Fang, R. (2012) Cucumber mosaic virus suppressor 2b binds to AGO4-related small RNAs and impairs AGO4 activities. *The Plant Journal*, 69, 104–115.

Han, Y.H., Xiang, H.Y., Wang, Q., Li, Y.Y., Wu, W.Q., Han, C.G. et al. (2010) Ring structure amino acids affect the suppressor activity of melon aphid-borne yellows virus P0 protein. *Virology*, 406, 21–27.

Himber, C., Dunoyer, P., Moissiard, G., Ritzenthaler, C. and Voinnet, O. (2003) Transitivity-dependent and -independent cell-to-cell movement of RNA silencing. *The EMBO Journal*, 22, 4523–4533.

Iki, T., Tschopp, M. and Voinnet, O. (2017) Biochemical and genetic functional dissection of the P38 viral suppressor of RNA silencing. *RNA*, 23, 639–654.

Kozlowska-Makulska, A., Guilley, H., Szyndel, M.S., Beuve, M., Lemaire, O., Herrbach, E. et al. (2010) P0 proteins of european beet-infecting poleroviruses display variable RNA silencing suppression activity. *Journal of General Virology*, 91, 1082–1091.

Kreuze, J.F., Souza-Dias, J.A.C., Jeevalatha, A., Figueira, A.R., Valkonen, J.P.T. and Jones, R.A.C. (2020) Viral diseases in potato. In: Campos, H. and Ortiz, O. (Eds.) *The Potato Crop*. Springer, Cham: Switzerland, pp. 389–430.

Lakatos, L., Csorba, T., Pantaleo, V., Chapman, E.J., Carrington, J.C., Liu, Y.P. et al. (2006) Small RNA binding is a common strategy to suppress RNA silencing by several viral suppressors. *The EMBO Journal*, 25, 2768–2780.

Li, Y., Sun, Q., Zhao, T., Xiang, H., Zhang, X., Wu, Z. et al. (2019) Interaction between brassica yellows virus silencing suppressor P0 and plant SKP1 facilitates stability of P0 *in vivo* against degradation by proteasome and autophagy pathways. *New Phytologist*, 222, 1458–1473.

Liu, Y., Zhai, H., Zhao, K., Wu, B., Wang, X. and Wang, X. (2010) Two suppressors of RNA silencing encoded by cereal-infecting members of the family *Luteoviridae*. *Journal of General Virology*, 93, 1825–1830.

Mangwende, T., Wang, M.L., Borth, W., Hu, J., Moore, P.H., Mirkov, T.E. et al. (2009) The P0 gene of sugarcane yellow leaf virus encodes an RNA silencing suppressor with unique activities. *Virology*, 384, 38–50.

Mérai, Z., Kerényi, Z., Molnár, A., Barta, E., Válóczi, A., Bisztray, G. et al. (2005) Aureusvirus P14 is an efficient RNA silencing suppressor that binds double-stranded RNAs without size specificity. *Journal of Virology*, 79, 7217–7226.

Mercado Central de Buenos Aires (2018) *Publicaciones técnicas*. Available at: http://www.mercadocentral.gob.ar/publicaciones/papa Accessed 1 September 2020

Mondal, S., Wenninger, E.J., Hutchinson, P.J.S., Whitworth, J.L., Shrestha, D., Eigenbrode, S.D. et al. (2017) Responses of aphid vectors of potato leaf roll virus to potato varieties. *Plant Disease*, 101, 1812–1818.

Nahirñak, V., Rivarola, M., Almasia, N.I., Barrios Barón, M.P., Hopp, H.E., Vile, D. et al. (2019) Snakin-1 affects reactive oxygen species and ascorbic acid levels and hormone balance in potato. *PLoS One*, 14, e0214165.

Nakamura, S., Mano, S., Tanaka, Y., Ohnishi, M., Nakamori, C., Araki, M. et al. (2010) Gateway binary vectors with the bialaphos resistance gene, *bar*, as a selection marker for plant transformation. *Bioscience, Biotechnology and Biochemistry*, 74, 1315–1319.

Pazhouhandeh, M. (2007) *The mechanism of action of polerovirus P0 in RNA silencing suppression*. PhD thesis, Universite Louis Pasteur, Strasbourg.

Pazhouhandeh, M., Dieterle, M., Marrocco, K., Lechner, E., Berry, B., Brault, V. et al. (2006) F-Box-like domain in the polerovirus protein P0 is required for silencing suppressor function. *Proceedings of the National Academy of Sciences of the United States of America*, 103, 1994–1999.

Qu, F., Ren, T. and Morris, T.J. (2003) The coat protein of turnip crinkle virus suppresses posttranscriptional gene silencing at an early initiation step. *Journal of Virology*, 77, 511–522.

Rashid, M., Zhang, X., Wang, Y., Li, D. and Yu, J. (2019) The three essential motifs in P0 for suppression of RNA silencing activity of potato leafroll virus are required for virus systemic infection. *Viruses*, 11, 170–185.

Ruiz, T.M., Voinnet, O. and Baulcombe, D.C. (1998) Initiation and maintenance of virus-induced gene silencing. *The Plant Cell*, 10, 937–946.

Schuck, J., Gursinsky, T., Pantaleo, V., Burgyá, J. and Behrens, S.E. (2013) AGO/RISC-mediated antiviral RNA silencing in a plant in vitro system. *Nucleic Acids Research*, 41, 5090–5103.

Vaucheret, H. (2008) Plant ARGONAUTES. *Trends in Plant Science*, 13, 350–358.

Wang, F., Zhao, X., Dong, Q., Zhou, B. and Gao, Z. (2018) Characterization of an RNA silencing suppressor encoded by maize yellow dwarf virus-RMV2. *Virus Genes*, 54, 570–577.

Wang, K.D., Empleo, R., Nguyen, T.T.V., Moffett, P. and Sacco, M.A. (2015) Elicitation of hypersensitive responses in *Nicotiana glutinosa* by the suppressor of RNA silencing protein P0 from poleroviruses. *Molecular Plant Pathology*, 16, 435–448.

Zaheer, K. and Akhtar, M.H. (2016) Potato production, usage, and nutrition – a review. *Critical Reviews in Food Science and Nutrition*, 56, 711–721.

Zhuo, T., Li, Y.Y., Xiang, H.Y., Wu, Z.Y., Wang, X.B., Wang, Y. et al. (2014) Amino acid sequence motifs essential for P0-mediated suppression of RNA silencing in an isolate of *Potato leafroll virus* from Inner Mongolia. *Molecular Plant-Microbe Interactions*, 27, 515–527.

SUPPORTING INFORMATION

Additional supporting information may be found online in the Supporting Information section.